

# Numerical Analysis of Adhesively Bonded Single Lap Joint



Author

Muhammad Hassan

319475

Supervisor

Dr. Aamir Mubashar

DEPARTMENT MECHANICAL ENGINEERING  
SCHOOL OF MECHANICAL & MANUFACTURING ENGINEERING  
NATIONAL UNIVERSITY OF SCIENCES AND TECHNOLOGY  
ISLAMABAD

JUNE 2022

# Numerical Analysis of Adhesively Bonded Single Lap Joint

Muhammad Hassan

319475

A thesis submitted in partial fulfillment of the requirements for the degree of  
MS Mechanical Engineering

Thesis Supervisor:

Dr Aamir Mubashar

Thesis Supervisor's Signature: \_\_\_\_\_

DEPARTMENT OF MECHANICAL ENGINEERING  
SCHOOL OF MECHANICAL & MANUFACTURING ENGINEERING  
NATIONAL UNIVERSITY OF SCIENCES AND TECHNOLOGY,  
ISLAMABAD  
JUNE, 2022

## **Declaration**

I certify that this research work titled “*Numerical Analysis of Adhesively Bonded Single Lap Joint*” is my work. The work has not been presented elsewhere for assessment. The material that has been used from other sources has been properly acknowledged/referred to.

Signature of Student

Muhammad Hassan

2019-NUST-MS-Mech-000319475

## Plagiarism Certificate (Turnitin Report)

This thesis has been checked for Plagiarism. Turnitin report endorsed by Supervisor is attached.

---

### ORIGINALITY REPORT

---

**15%**

SIMILARITY INDEX

**8%**

INTERNET SOURCES

**12%**

PUBLICATIONS

**1%**

STUDENT PAPERS

---

Signature of Student

**Muhammad Hassan**

**Reg. #: 00000319475**

Signature of Supervisor

## **Copyright Statement**

- Copyright in the text of this thesis rests with the student author. Copies (by any process) either in full or of extracts, may be made only by instructions given by the author and lodged in the Library of NUST School of Mechanical & Manufacturing Engineering (SMME). Details may be obtained by the Librarian. This page must form part of any such copies made. Further copies (by any process) may not be made without the author's permission (in writing).
- The ownership of any intellectual property rights which may be described in this thesis is vested in NUST School of Mechanical & Manufacturing Engineering, subject to any prior agreement to the contrary, and may not be made available for use by third parties without the written permission of the SMME, which will prescribe the terms and conditions of any such agreement.
- Further information on the conditions under which disclosures and exploitation may take place is available from the Library of NUST School of Mechanical & Manufacturing Engineering, Islamabad.

## **Acknowledgements**

First of all, I am thankful to ALLAH Almighty, who gave me knowledge and dedication to be able to complete this research.

I am greatly pleased to express my profound gratitude and heartfelt thanks to my supervisor Dr. Aamir Mubashar for his excellent guidance, expert advice, and strong support during the entire period of research.

*Dedicated to my exceptional parents and adored siblings whose  
tremendous support and cooperation led me to this wonderful  
accomplishment.*

## Abstract

This research shows the effect of aluminum oxide  $\text{Al}_2\text{O}_3$  nanoparticles included in Epocast 50-A1/946 epoxy adhesive at different temperatures in quasi-static tensile loading. The single lap adhesive joint with two different types of material adherends was used: composite fiber reinforced plastic and aluminum 5083 adherends. The effect on peel stress and shear stress was compared by adding  $\text{Al}_2\text{O}_3$  nanoparticles into the neat adhesive at 25°C, 50°C, and 75°C temperatures at four locations of the adhesive region: the top face (interface of aluminum and adhesive), the middle plane of adhesive, the longer edge (along the length of adhesive), the shorter edge (along the width of adhesive). The results show that adding nanoparticles into the neat adhesive improves the strength of the joint at room and elevated temperatures. High peel stress and shear stress were recorded near both edges of the top face (interface). At the top face, the peak peel stress was reduced by 1.3% and increased by 2.7% and 10.7% for 25°C, 50°C, and 75°C temperatures respectively and the same trend was observed for other locations. At the top face, the peak shear stress decreased by 19.6% and increased by 7.7% and 8.7% for 25°C, 50°C, and 75°C temperatures respectively and the same trend was observed for other locations. It was noted that adding aluminum oxide nanoparticles made adhesive stiffer at higher temperatures and made it more applicable to bear more force. Moreover, it was also noted that the peak of stress lies near the edges, indicating that the crack will most probably start close to the edges along the length of adhesive and translate towards the center and causes ultimate failure.



# Table of Contents

<b>Declaration</b> .....	<b>i</b>
<b>Plagiarism Certificate (Turnitin Report)</b> .....	<b>i</b>
<b>Copyright Statement</b> .....	<b>ii</b>
<b>Acknowledgments</b> .....	<b>iii</b>
<b>Abstract</b> .....	<b>v</b>
<b>Table of Contents</b> .....	<b>vi</b>
<b>List of Figures</b> .....	<b>ix</b>
<b>List of Tables</b> .....	<b>xii</b>
<b>1. CHAPTER 1: INTRODUCTION</b> .....	<b>1</b>
1.1. Background .....	1
1.2. Research Gap.....	4
1.3. Problem Statement .....	4
1.4. Aims and Objectives .....	4
1.5. Research Scope .....	4
<b>2. CHAPTER 2: Literature Review</b> .....	<b>5</b>
2.1. Advantages and Disadvantages of Adhesive Joints .....	5
2.1.1. Advantages [14-18].....	5
2.1.2. Disadvantages [14-18] .....	5
2.2. Stresses in Adhesive Joints .....	6
2.2.1. Shear Stress .....	6
2.2.2. Tensile Stress .....	7

2.2.3.	Compressive Stress .....	7
2.2.4.	Cleavage Stress .....	7
2.2.5.	Peel Stress .....	7
2.3.	Types of Adhesive Joints .....	7
2.4.	Factors that affect the strength of adhesive joints .....	10
2.5.	Factors affecting CFRP and Aluminum Adhesive joints .....	13
2.6.	Influence of Temperature on the strength of adhesive joint.....	15
2.7.	Effect of Adding Nanoparticles into the Composite Adhesive Joint .....	17
<b>3.</b>	<b>Chapter 3: Finite Element Modeling.....</b>	<b>20</b>
3.1.	Introduction .....	20
3.2.	Initial Geometry Configuration .....	20
3.3.	Loading and Boundary Conditions .....	22
3.4.	Meshing Methodology and Element Formulation .....	22
3.5.	Type of Mesh Elements.....	24
3.6.	Validation of Finite Element Model.....	26
<b>4.</b>	<b>Chapter 4: Results and Discussion .....</b>	<b>29</b>
4.1.	Neat Adhesive SLJ.....	29
4.1.1.	At the Middle of Top Face (Interface).....	29
4.1.2.	At middle plane of adhesive .....	32
4.1.3.	At the longer edge of adhesive (along length) .....	33
4.1.4.	At the Shorter Edge of Adhesive (along width).....	35
4.2.	Adhesive Joint with Alumina Oxide (Al <sub>2</sub> O <sub>3</sub> ) Nanoparticles.....	37
4.2.1.	At the Top Face of adhesive (interface).....	37

4.3.	Comparison between Neat and Nano filler Adhesive .....	44
4.3.1.	Graphical Comparison of Peel Stress between Neat and Al <sub>2</sub> O <sub>3</sub> nanoparticles Adhesive	47
4.3.2.	Graphical Comparison of Shear Stress between Neat and Al <sub>2</sub> O <sub>3</sub> nanoparticles Adhesive	51
<b>5.</b>	<b>Chapter 5: Conclusion and Future Work.....</b>	<b>55</b>
5.1.	Conclusion.....	55
5.2.	Future Work .....	56
<b>6.</b>	<b>REFERENCES.....</b>	<b>57</b>

## List of Figures

Figure 1.1: Failure modes in a Single Lap joint [9].....	3
Figure 2.1: Stress Types in Adhesive Joints [20] .....	6
Figure 2.2: Peel Stress distribution in the adhesive layer of Single Lap Joint [21].....	8
Figure 2.3: Classification of Adhesive Joints [21].....	9
Figure 2.4: Geometry optimization of adhesive layer [31].....	12
Figure 3.1: Geometry of Single Lap Joint (Not to Scale).....	21
Figure 3.2: Boundary and Loading Conditions of Single Lap Joint SLJ (Not to Scale) .....	22
Figure 3.3: Partwise SLJ Meshing .....	25
Figure 3.4: Detailed Meshing of SLJ .....	26
Figure 3.5: C3D8R (An 8-node linear brick, 3D Stress Element) .....	26
Figure 3.6: Single Lap joint with composite adherends used for validation work .....	27
Figure 3.7: Comparison of Peel Stress in the middle of adhesive layer of SLJ between reference and present study.....	27
Figure 4.1: Path drawn at interface of Neat Adhesive and Aluminum for Peel Stress and Shear Stress Results .....	30
Figure 4.2: Peel Stress distribution at the interface of the overlap region of Neat-SLJ at different temperatures .....	30
Figure 4.3: Shear Stress distribution at interfacinof g the overlap region of Neat-SLJ at different temperatures .....	31
Figure 4.4: Path drawn at middle plane of Adhesive for peel stress and shear stress results .....	32
Figure 4.5: Peel Stress distribution at middle plane of adhesive at different temperatures .....	33
Figure 4.6: Shear Stress distribution at middle plane of adhesive at different temperatures.....	33
Figure 4.7: Path drawn at longer edge of Adhesive for peel stress and shear stress results .....	34

Figure 4.8: Peel Stress distribution at Length Side of adhesive at different temperatures .....	34
Figure 4.9: Shear Stress distribution at Length Side of adhesive at different temperatures .....	35
Figure 4.10: Path drawn at Width Side of Adhesive for peel stress and shear stress results.....	36
Figure 4.11: Peel Stress distribution at Width Side of adhesive at different temperatures .....	36
Figure 4.12: Shear Stress distribution at Width Side of adhesive at different temperatures .....	37
Figure 4.13: Path drawn at interface of Al <sub>2</sub> O <sub>3</sub> nano particle Adhesive and Aluminum for Peel Stress and Shear Stress Results .....	38
Figure 4.14: Peel Stress distribution at the interface of the overlap region of Al <sub>2</sub> O <sub>3</sub> nano particle-SLJ at different temperatures .....	38
Figure 4.15: Shear Stress distribution at interface the overlap region of Al <sub>2</sub> O <sub>3</sub> nano particle-SLJ at different temperatures .....	39
Figure 4.16: Path drawn at Inside of Al <sub>2</sub> O <sub>3</sub> nano particle Adhesive for peel stress and shear stress results .....	40
Figure 4.17: Peel Stress distribution at middle plane of adhesive with Al <sub>2</sub> O <sub>3</sub> nano particles at different temperatures .....	40
Figure 4.18: Shear Stress distribution at middle plane of adhesive with Al <sub>2</sub> O <sub>3</sub> nano particle at different temperatures .....	41
Figure 4.19: Path drawn at the longer edge of Al <sub>2</sub> O <sub>3</sub> nano particles- Adhesive for peel stress and shear stress results.....	42
Figure 4.20: Peel Stress distribution at the longer edge of adhesive with Al <sub>2</sub> O <sub>3</sub> nano particles at different temperatures .....	42
Figure 4.21: Shear Stress distribution at the longer edge of adhesive with Al <sub>2</sub> O <sub>3</sub> nano particle at different temperatures .....	42
Figure 4.22: Path drawn at Shorter Edge of Adhesive for peel stress and shear stress results.....	43
Figure 4.23: Peel Stress distribution at the shorter edge of adhesive with Al <sub>2</sub> O <sub>3</sub> nanoparticles at different temperatures .....	44

Figure 4.24: Shear Stress distribution at shorter edge of adhesive with Al <sub>2</sub> O <sub>3</sub> nanoparticle at different temperatures .....	44
Figure 4.25: Geometrical locations of adhesive where results are focused .....	46
Figure 4.26: Comparison of Peel Stress of Neat and Al <sub>2</sub> O <sub>3</sub> Nanoparticles Adhesive at Top Face	47
Figure 4.27: Comparison of Peel Stress of Neat and Al <sub>2</sub> O <sub>3</sub> Nanoparticles Adhesive at Middle Plane .....	48
Figure 4.28: Comparison of Peel Stress of Neat and Al <sub>2</sub> O <sub>3</sub> Nanoparticles Adhesive at Longer Edge (Along Length).....	49
Figure 4.29: Comparison of Peel Stress of Neat and Al <sub>2</sub> O <sub>3</sub> Nanoparticles Adhesive at Shorter Edge (Along Width).....	50
Figure 4.30: Comparison of Shear Stress of Neat and Al <sub>2</sub> O <sub>3</sub> Nanoparticles Adhesive at Top Face .....	51
Figure 4.31: Comparison of Shear Stress of Neat and Al <sub>2</sub> O <sub>3</sub> Nanoparticles Adhesive at Middle Plane.....	52
Figure 4.32: Comparison of Shear Stress of Neat and Al <sub>2</sub> O <sub>3</sub> Nanoparticles Adhesive at Longer Edge (Along Length) .....	53
Figure 4.33: Comparison of Shear Stress of Neat and Al <sub>2</sub> O <sub>3</sub> Nanoparticles Adhesive at Shorter Edge (Along Width).....	54

## List of Tables

Table 3-1: Material Properties of Al 5083, Neat adhesive, and adhesive with Al <sub>2</sub> O <sub>3</sub> nano particles [56].....	21
Table 3-2: Material Properties of T300/QY8911 CFRP Composite Lamina [59].....	21
Table 4-1: Comparison of Percentage Change in Peel stress and Shear Stress with inclusion of 1.5wt% Al <sub>2</sub> O <sub>3</sub> Nanoparticles in Epocast 50-A1 Adhesive.....	46

## CHAPTER 1: INTRODUCTION

The research study in the present dissertation is addressing the numerical analysis of 3D modeled composite single lap adhesive joint. The objective of the research is to study the effect of temperature variation and nanoparticle concentration on the strength and stresses of the joint at different locations on adhesive. To analyze the effect of these factors, the composite single lap joint is subjected to Quasi-Static tensile loading in Abaqus CAE.

### 1.1. Background

There are several reasons both objective and subjective for the popularity of adhesive joints as primary choice for connecting different parts [1]. The important part of the adhesive joint is the adhesive itself which is used to joint different or similar material parts together. For that, the availability of adhesive is in thousands with subtle and significant differences. The possibility of joining various materials together is unimaginable because of the different types of adhesive available. Nowadays the world is shifting towards the adhesive as the primary source to connect different parts of the same or different material. The application of adhesive includes computers, auto parts, aerospace industry, mobile phones, medical devices marine industry, construction industry [2].

There are several characteristics that adhesive joints have which is the reason for their importance. The characteristic includes low weight, high stiffness, and high strength and it has very low cost compared to conventional mechanical joints [3]. The determination of adhesive bonded joints efficiency is essential and by various aspects, it can be determined such as the surface treatment used in the adherends' surfaces development [4]. The mechanical strength of adhesive joint is the most essential aspect and characteristic that needs consideration at first while studying or applying adhesives. It has a direct connection to other properties of the adhesive joint. There is active research going on in different parts of the world focusing on the different test and numerical procedure to determine the strength of adhesive joint especially when two different material is connected together like carbon fiber reinforced plastic bonded together with aluminum.

There are various of possibilities of joints such as Single Lap Joints SLJ, Double Lap Joints, step joints, and scarf joints [5]. There is an abundant of literature filled with experimental and numerical



analyses of these types of adhesive joints [6]. But the present research is focused on the single lap adhesive joints (SLJ). The strength of SLJ is dependent of various factors. All the factors have different effects on the strength. The factors include adhesive type, which can be ductile or brittle, weak or strong, length of the overlap between the adherends, generally this region is where the adhesive is used for bonding, adherend type, thickness of adherend, thickness of adhesive, joint geometry, temperature, nanoparticle concentration. All these factors affect the strength of the adhesive joint and experimental and numerical studies help access them. The present research incorporates a detailed literature review focusing on the numerical studies conducted for studying the strength of the joint and other parameters. Based on the literature, a numerical technique is adopted for this research.

The effect of overlap length and adherend thickness on failure mode and strength of Carbon Fiber Reinforced Plastic CFRP single lap joint was analyzed in research [7]. Phase angle decrease as effective length grows for joint having small overlaps and increases for joint having larger overlaps. The maximum load is also affected by the overlap length as in research [8]. It has shown substantial dependent on length of overlap of a double strap joint. It was shown that two-fold increase in overlap length (50mm to 100mm) cause the increase of 50% in max. load. It was observed that shear strength of SLJ is more effected by overlap length than the thickness. The strength of CFRP and aluminum SLJ was analyzed for different strain rates. Brittle failure occurred in CFRP of the SLJ at high strain rates.

The failure modes in an adhesive joint are of three types: cohesive failure, adhesive failure, and mixed failure [9], following figure 1.1 also show failure modes. These failure modes are influenced by the strength of adhesive bond at contacts. The effect of increasing the strain rate influence the failure mode transmission like the adhesive failure transform into cohesive failure. The fiber tear in the CFRP is difficult to anticipate since joint making process, adhesive epoxy, temperature, and other factors also influence the failure mode [10].

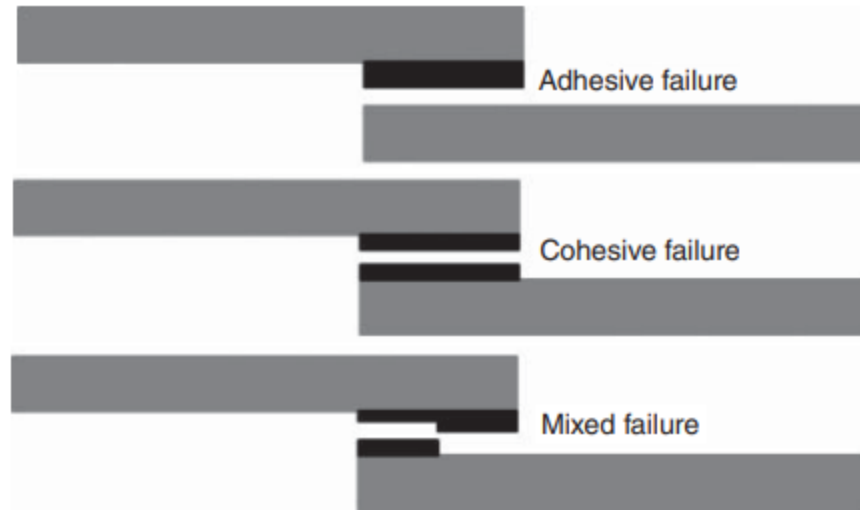


Figure 1.1: Failure modes in a Single Lap joint [9]

The research in the literature shows that joint strength is affected by the temperature factor. The characteristic of BFRP-Al adhesively bonded joint specifically the strength of the adherend and adhesive is greatly affected by temperature variation. BJs, SJs and TASJs record reduction in strength at high temperature [11]. The modulus and strength of adhesive joint is high if temperature is less than the glass transition temperature ( $T_g$ ). But it is tough and flexible against the temperature more than transition temperature but loses the strength. The properties of the adhesive bond are greatly affected by the temperature variation.

The strength of the adhesive joint can be improved by inclusion of nanoparticles into the adhesive by a small weight age compared to adhesive. The composition, size, shape, type and density of nanoparticles are critical in selecting the nanoparticle to get optimum qualities in epoxy adhesive [12]. The inclusion of nanoparticles into adhesive epoxy showed significant improvement in adhesive's mechanical performance like tensile resistance improved by 18%, at rupture the strain energy improved by 53%. These results were shown in research [13].

In the present research the effect of temperature and the inclusion aluminum oxide  $Al_2O_3$  nanoparticle is studied numerical in Abaqus CAE. The temperature variation range is from  $25^\circ C$  to  $100^\circ C$ . The aluminum oxide concentration is also varied in the process. There are two different adherends one is aluminum material, and the other is a bi-directional CFRP. The sole purpose of the analysis is to evaluate the SLJ's strength under tensile loading.

## **1.2. Research Gap**

- a) The strength of adhesive joint is greatly affected by introducing temperature variation and by conducting the literature review, there is limited research found where the temperature effect is numerically investigated.
- b) When nanoparticles, carbon nanotubes, and cork powder are added in a precise amount, they boost the strength of adhesive joints.
- c) The synergistic impact of temperature and  $\text{Al}_2\text{O}_3$  addition on joint strength is mainly unknown and limited finite element analyses are found in the literature.

## **1.3. Problem Statement**

The strength of single lap joints is strengthened by introducing nanoparticle of aluminum oxide at room temperature. However, joints may experience temperature changes over their operational life. The durability of single joints at different temperatures and nanoparticle concentrations is unknown.

## **1.4. Aims and Objectives**

The aim of this research is to investigate the strength and failure load of single lap joints at various temperatures and nanoparticle concentrations. The following objectives were identified to attain the aim.

- (a). To analyze the peel stress and shear stress at four different locations on the adhesive layer.
- (b). To compare the effect of adding  $\text{Al}_2\text{O}_3$  nanoparticles into neat adhesive at different temperatures.
- (c). To analyze the response of neat and  $\text{Al}_2\text{O}_3$  nanoparticles adhesive upon tensile loading.

## **1.5. Research Scope**

- a) The adherends used in my research consists of two different material that is Aluminum 5083 and composite carbon fiber reinforced plastic CFRP adherends.
- b) The adhesive consists of epoxy that is
- c) The analysis was conducted at different temperatures and  $\text{Al}_2\text{O}_3$  nanoparticles
- d) 3D model Composite single lap joint was constructed in Abaqus CAE.

## **CHAPTER 2: Literature Review**

### **2.1. Advantages and Disadvantages of Adhesive Joints**

This chapter covers the detailed review of literature regarding adhesive joint and narrow down to literature on present research study. It starts with advantages and dis-advantages of adhesive bonded joints

#### **2.1.1. Advantages [14-18]**

- Manufacturing is relatively easy and incur low cost.
- Compared to conventional joints (joints by nuts and bolts, rivet etc.) materials of any shapes can be bonded together especially thin shapes materials.
- Provides comparatively uniform stress distribution unlike conventional joints where there are more chances of stress concentration points.
- Provides higher strength with less weight characteristics.
- Different materials can be joined easily known as composite adhesive joints.
- These types of joints provide much better resistance to fluctuating loads and fatigue.
- Provides protection against vibration and have better ability to absorb shocks.
- Minimize galvanic corrosion in composite joints (adherends of different materials bonded together).
- Provides better resistance to heat effects on bonded adherends which is mostly observed in welded joints.

#### **2.1.2. Disadvantages [14-18]**

- Requires surface treatment before bonding.
- In adhesive bonding the inspection is difficult.
- Adhesive bonding takes more time to cure.
- Jigs and fixtures are needed to bond the substrates properly.
- Applicable life of adhesive joints is depended upon service environment.
- Consideration of environmental, health and safety are important because chemical are used in the surface treatment.

- The service temperature of adhesive bonding is usually limited typically to the range of 170°C - 200°C.

## 2.2. Stresses in Adhesive Joints

There are many types of stresses that appear in the adhesive joints when subjected to various types of loadings. These are shown in the figure 2.1. Generally, adhesive joint experience types of stresses like tensile stress, compressive stress, cleavage, shear and/or peel stress. These types of stresses can be inherited by adhesive joints in combination of the types mentioned above. To understand the types of stresses that appear in the joints, they are explained separately as follows.

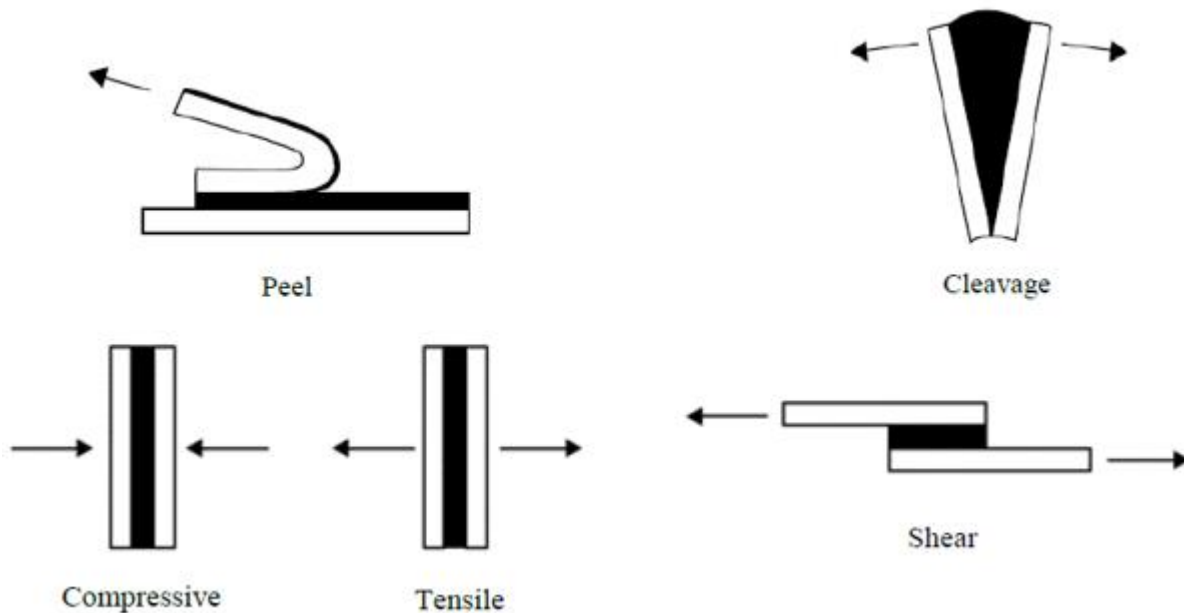


Figure 2.1: Stress Types in Adhesive Joints [20]

### 2.2.1. Shear Stress

This type of stress appears in the joint when subjected to eccentric loading. Due to stress distribution across whole bond region, shear stress uses the entire area making the joint economical and more resilient to failure. Therefore, the joint should be arranged in a way that the load is carried by shear component of the stress. Thus shear load is more desirable to be applied on the adhesive joints [19, 20].

### **2.2.2. Tensile Stress**

This type of stress appears in the joint if pulled perpendicularly to the bonded region and in doing so the stress is evenly distributed over the adhesive region. The advantage of even stress distribution is lost if the tensile force loses the perpendicularity by a slight degree. Consequently, increasing the probability of losing resistance to failure. The joint subjected to shear loading and tensile loading is highly comparable as even distribution of stress is a common behavior of the joint [19, 20].

### **2.2.3. Compressive Stress**

Compressive stress appears in the joint due to compression of the bonded area. In this type of stress, the occurrence of failure in the joint is very low when compared to tensile and bending loads. The practical application of the adhesive joint subject to compression is limited [19, 20].

### **2.2.4. Cleavage Stress**

Cleavage stress appears in the joint when an offset tensile force or bending moment is applied. Unlike to the cases discussed above, there is no even distribution of stress but the stress is concentrated at one end of the adhesive region. To accommodate cleavage stress in the joint, a large area of the bonded region is required making the adhesive joint less economical [19, 20].

### **2.2.5. Peel Stress**

Peel stress appears in the joint if joint is subjected to tensile with offset line of force or peeling. For this type of stress, one or both adherends must have behavior of flexible material. The stress is higher along the boundary line of the joint due to effect of peel and unless the applied load is small or joint area is large, probability of failure is high [19, 20].

## **2.3. Types of Adhesive Joints**

Unlike conventional joint, adhesive is used between to metal plates sometime known as adherends. The basic types of adhesive joints are named as Butt Joint, Lap Joints, Strap Joints. These joints are further divided depending upon the use of the joints, the classification is shown in Figure 2.3 [21]. In all the classified adhesive joints, butt joint is the simplest and easy to make, two flat

surfaces are bonded together with an adhesive. However, applying bending loads on this type of joints is not desirable strength wise due to cleavage stress appearing in the adhesive. The other types of butt joints help improve in strength and reduction of cleavage stresses in the adhesive region. For example, the tough and groove joint is quite remarkable in strength, and it also helps in self-alignment and act as reservoir for the adhesive. So, these modifications can be an alternate design for the simple butt joint in improving strength and resisting cleavage stresses. [21, 22]. Alves and Campilho [14] numerical and experimentally investigated the effect of different scarf angle  $\alpha$  and adhesive on a composite scarf joint (composite and aluminum adherend). The result of this investigation shows that scarf angle  $\alpha$  and type of adhesive impacted the joint behavior significantly.

The easiest to manufacture and mostly used is lap joint. In lap joint the metal adherends are bonded with adhesive on top of one another, having some overlap area. In these type of joints shear stresses occur majorly when the metal adherends are pulled away, especially peel stresses in single lap joints. As the single lap joints are eccentric, they tend to get peak peel stresses at end of overlap regions as shown Figure 2.2. It can be seen that stress concentration is higher at the end of overlap regions whereas comparatively low stress at center overlap region.[20, 21]

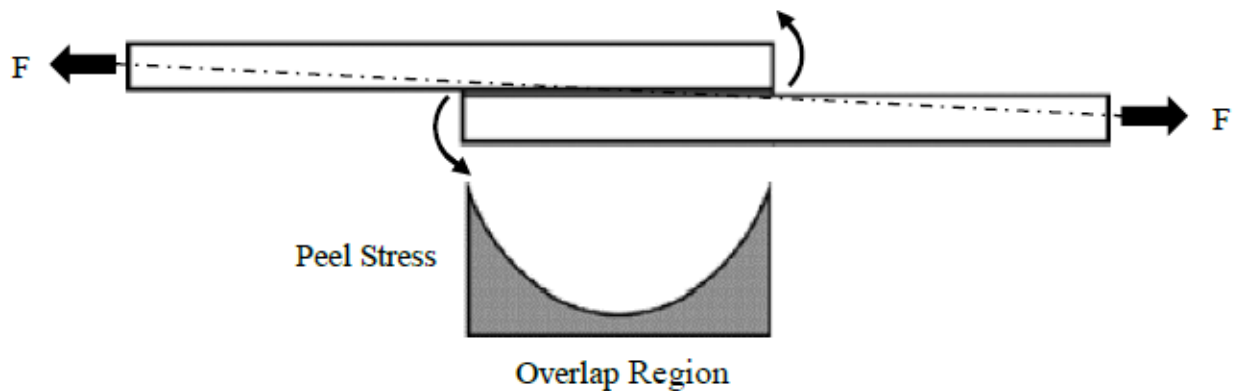


Figure 2.2: Peel Stress distribution in the adhesive layer of SLJ [21]

### Butt Joints



Simple Butt Joint - Not Satisfactory



Scarf Butt Joint – Good, Generally Practical

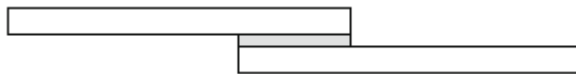


Double Butt Lap Joint – Good, Needs Machining

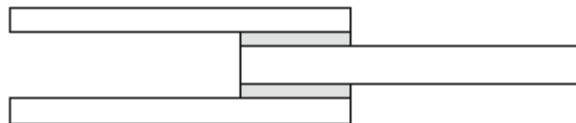


Tongue And Groove Butt Joint Excellent, Needs Machining

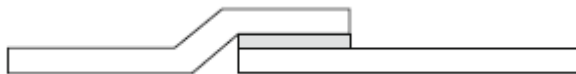
### Lap Joints



Single Lap Joint (SLJ) – Good, Very Practical



Double Lap Joint – Very Good, Difficult to Manufacture, Practical

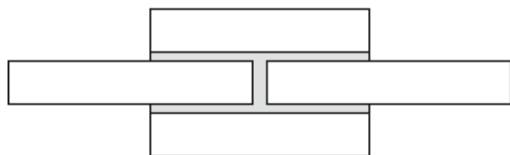


Joggle Lap Joint – Good, Practical

### Strap Joints



Single Strap Joint – Fair, Sometimes Desirable



Double Strap Joint – Good, Sometimes Desirable



Recessed Double Strap Joint – Very Good, Expensive & to Machine

Figure 2.3: Classification of Adhesive Joints [21]



Strap joint and butt joint are similar but single strap is added as in case of single strap joint and two straps as in case of double strap joint. Due to eccentricity of loading leading to elevated peel stress at the edges of overlap area, single strap joint is at disadvantage which is similar to the behavior of single lap joint. Double strap joint is much stronger in this prospect as two straps nullify the bending moment effect however the joint is difficult to make and increase weight of overall structure [21, 22].

## **2.4. Factors that affect the strength of adhesive joints**

An adhesive layer with uniform distribution of stress in an adhesive joint has much more usage advantage than convention joints as discussed earlier. But achieving perfection stress distribution is not possible which open room for improvement in the joints. From the discussion above, it can be seen that peel and cleavage stresses are highly the cause of failure in adhesive joints. So, various studies have been conducted to counter this issue and give a way forward to improve the strength of adhesive joints. This section focuses on the literature of factors that are crucial in affecting the strength of adhesive joints. And analyze how the strength can be increased in different conditions.

E.M. Moya-Sanz et al. [23] studied several configurations based on geometry of single lap joint (SLJ) to analyze the variation in strength of the joint by changing geometry. The geometry configuration includes chamfering adherends, adherend and adhesive recessing. To observe the strength, factors including adherend's vertical displacement, peel stress distribution along overlap region and failure load was analyzed and it was concluded that chamfering the adhesive and adherend at  $15^\circ$  has greatly influence the strength of adhesive joint and was the best option. Decreasing chamfer angle, increase the failure of the adhesive joint and reduced the peak peel stress and vertical displacement in the adhesive joint.

W. Guo et. al. [24] numerically explored and proposed a new model varying thickness bond line of adhesive joints. Cohesive Zone Model (CZM) was used to numerically analyze three surface roughness options including trapezoidal, triangular, and circular protuberances. Interface damage, fracture energy and ultimate load were calculated and considering the geometric parameters of protuberance interfacial defects and adhesive types were comprehensively studied. Their study shows that strength can be improved by properly controlling the geometric parameters of

protuberance as their results shows change in load bearing capacity because of change in adhesive thickness due to the effect of protuberance.

A similar study was conducted by P.Chen et. al. [25] by analyzing graded adherends subjected to uniaxial tensile load for interfacial behavior and strength of SLJ. Peak loading and fracture energy were their primary focus and result showed that choosing proper geometry parameters and material for adhesive joints will result in improving fracture energy and peak load. Their study also shows that SLJ strength is much more dependent on soft region near adhesive layer of the joint.

Adams Peppiatt [26] studied metal to metal single lap adhesive joint for stress distribution by using 2D FEM. They conclude that the max. principal stress magnitude decreases by 40% by adding 45 triangular spew fillets at end of overlap region. Adams and Haris [27] also investigated spew fillet effect on strength of aluminum SLJ. They concluded that 50% of increase in strength of joint by adding fillet adhesive.

Ferreria et. al. [28] carried experimental and numerical analysis to analyze the different T-stiffeners under peeling loads. Their work used araldite 2015 structural adhesive and composite adherends. Four geometrical parameters were considered including stiffener thickness, overlap length, adherend thickness for elastic stress analysis and max load prediction. All the parameters have significant effect on the strength of joints. Liu and Sawa [29] conducted a study on dissimilar joints bonded adhesively analyzing stress distribution by using 2D plain strain problem. Effect of adherend's elastic modulus, adherend thickness and length ratio on distribution of stress at interfaces were examined. It was noted that stress singularity appeared in the case with adherend of smaller elastic modulus and it was more prone to occur at the interfaces.

Adams and Atkins et al [30] studied for the strength of adhesive joints. Particularly for double lap joint in which carbon fiber reinforce plastic CFRP was used as center adherend while the other two were of steel. In their study, based on numerical and experimental analysis, result showed that adhesive joint strength has increased three folds by including external and internal taper with adhesive fillet. Martin and Sandu et al [31] investigated deformation and stress in the single lap strap joint having adherends of tapered and squared experimentally and numerically. It was concluded that max. stress is significantly reduced by tapering the adherends in overlap area of the adhesive joint.

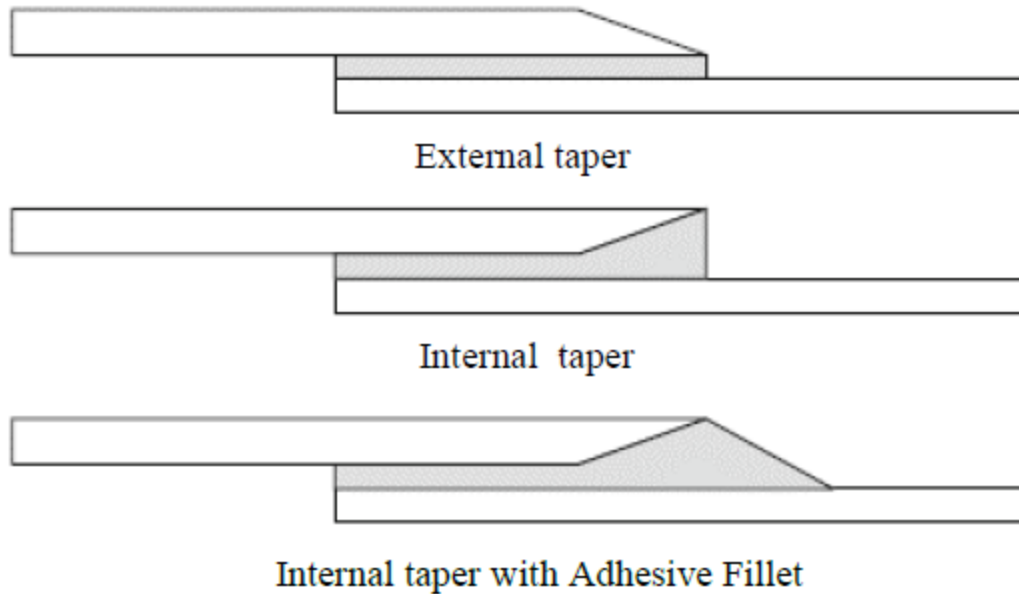


Figure 2.4: Geometry optimization of adhesive layer [31]

Lucas da Silva [32] investigated the strength of adhesive joint incorporating mixed adhesive. In the previous studies it was evident that using brittle adhesive in the middle and ductile adhesive at the ends gives strength to the joint. SLJ was manufactured and tested duplicating the same configuration of brittle material adhesive in middle area and three different types of ductile material adhesive at both ends. Prediction of strength of joint was proposed in their study. It was observed that using mixed adhesive material joints show improvement in strength than using brittle material adhesive in the joint. For joint with mixed material adhesive stronger than ductile material and brittle material joint alone, the load carrying capability of brittle material adhesive must be greater than ductile material adhesive.

Kimiyoshi Naito [33] investigated the adhesive thickness effect on shear strength and tensile strength. the test were carried out on single lap and butt joint. The adhesive and adherend used were polyimide (Skybond 703) and aluminum (5052-H34) respectively. The results showed decrease in tensile strength as the thickness of adhesive was increased but this change did not effect shear strength. the failure was interfacial manner whatever the thickness of adhesive was. According to FEM linear elastic stress analysis there was concentration of normal stress between adhesive and adherend. Conducting FEM analysis considering stress at interfaces add to understand the effect of thickness of adhesive on strength of joint.

## 2.5. Factors affecting CFRP and Aluminum Adhesive joints

Ligang and Cheng [34] investigated composite adhesive joints subjected to tensile loading. Their study focused on changing various geometric parameters and see their performance against tensile loads. The geometric parameters include overlap lengths (7 specimens), width of adherends (5 specimens), stacking sequence (3 specimens). The tensile behavior on single lap composite adhesive joint was analyzed using 3D FEMs. In their study, it was concluded that changing the adherend width of the joint has more effect load carrying capability of the joint than changing overlap length. It was also viewed that while constructing CFRP substrate first ply should be  $0^\circ$  to take the strength of the joint one step further. Their study shows that SLJ having CFRP layup of  $[0/45/-45/90]_{3S}$  are more likely to have cohesive failure whereas SLJ having CFRP layup of  $[90/-45/45/0]_{3S}$  more prone to delamination. Araújo and Machado [35] investigated composite adhesive joints behavior under impact loading. The adhesive used in joining two different material adherends was ductile epoxy adhesive. It was concluded that such type of adhesives and combining two dissimilar adherends one particularly CFRP exhibits exceptional damping capabilities and impact strength. In their research, vibrational analysis was used for dynamic test to study damping capabilities.

Banea and Rosioara [36] investigated adhesive joints of multi-material experimentally and numerically. The materials that were used to form adhesive joints are Hard Steel (HS), Aluminum (Al) and CFRP i.e., CFRP/Al and CFRP/HS. Factors like stiffness of adherends, overlap length effecting the strength of composite adhesive joints were analyzed. The results showed that material and/or geometry combination effect is not significant on the strength of joint. Whereas failure in the SLJs having relative small overlap lengths dominated by global yielding of adhesive.

Campilho and Moura [37] investigated residual strength and stress distribution of a refurbished composite plate under tensile load. The important parameters about good performance were patch thickness, geometry of the specimen and stacking sequence. Numerically, different failure modes were considered along with effect of layers properties adhesive/adherend and patch/adhesive interfaces in those modes were investigated. Their results showed that adhesive strength has important effect on mode of failure whereas interface and adhesive fracture toughness has little effect.

Wang and Liang [38] investigated influence of rate of loading on failure mode and mechanical properties of CFRP and Aluminum (Al) alloy SLJ. For shear test, different rates of loading were used including 0.12, 4, 8 and 12 m/s. Strain evolution were analyzed using a technique called Digital Image Correlation (DIC). Their results shows that shear strength of the composite adhesive joint increased with increasing rate of loading. Statistically average increase in strength was recorded from 19.3 MPa to 29.2 MPa when the loading rate was increased from 0.12 m/s to 12 m/s. There were two types of failure recorded naming fiber tear failure and cohesive failure. Cohesive failure was caused by development of stress concentration at the ends of adhesive joint region whereas fiber tear failure mode was mainly occurred in the middle of the joint area highly likely failure of resin mixture of CFRP.

Morgado and Carbas [39] investigated the problem of adhesive delamination in the composite adhesive single lap joints. They studied on reduction of delamination by inserting adhesive layer in adherends used in bonding. Experimental investigation was for quasi-static loading and impact conditions. It was viewed an increase in failure load as well as delamination was averted in quasi-static analysis. Wenlong and Guofeng [40] investigated a hygro-thermally aged joint. In their investigation the effect of variable loads on the residual strength on the joint was focused. The results showed that strength of the adhesive joint was heavily damaged and decreased when exposed to hygro-thermal aging. When the joint is subjected to variable loading decrease in strength was observed apparently quicker in higher loads.

Monika and Jarosław [41] investigated the comparison of pretreatment of surface and fibers configuration in fiber metal laminate FML. FML was based on carbon fibers and aluminum with glass. Type of fiber used and pretreatment of the surface of adhesive joint were decisive in adhesive joint strength and cohesive failure. Reis and Ferreira [42] did a comparative study on shear strength of SLJs with different material adherends. Composite, steel and aluminum adherends were combine in different combinations. Adherend stiffness was the major factor influencing the shear strength of the joints. Depending on the material of adherends, overlap length in the adhesive joints also affected the shear strength.

Ribeiro and Campilho [43] experimentally and numerically studied composite adhesive joint i.e., joint between carbon epoxy and aluminum. The factors that were considered in the study were overlap length ( $L_o$ ) and different types of adhesives. The failure process was described using crack

growth and damage analysis. The influence of joint strength was highly dependent upon type of adhesive. Brittle adhesive showed nearly negligible improvement in the peak load ( $P_m$ ) whereas linear improvement was observed when adhesive of ductile nature was used.

Jakub and Andrzej [44] investigated the environmental effects on the shear and tensile strength of the composite adhesive joints. Composite joints were composed CFRP and aluminum of different grade: high strength and resistant to abrasion. Two different types of adhesives were also considered in their analysis: adhesive for moderate temperature and adhesive for elevated temperatures. Complying to the SAE standards humidity-temperature cycle test were conducted to access conditions. The results showed that debonding in the adhesive occur in the humid and high temperature conditions even if there were no external force applied. According to the numerical analysis thermal expansion coefficient of the adhesive was major factor which highly influenced the performance of the joints in presented conditions.

Jairaja and Narayana [45] investigated dual adhesive in SLJ of different adherends. It was known that strength of adhesive joint depends on adhesive type and its properties. It has more importance in composite adhesive joints such as CFRP and aluminum which was under study by them. They used two adhesives namely Araldite 2015 and AV138 separately as well as in combination. In combination, the adhesive that has ductile properties must be at the ends whereas brittle adhesive must in the middle that is what they have done. According to their results using two adhesives in combination as described helped in getting higher strength of the composite adhesive joints.

## **2.6. Influence of Temperature on the strength of adhesive joint**

Rahmani and Choupani [46] investigated the aluminum-aluminum adhesive joints at different low temperatures for fracture parameters. The results showed that at low temperatures the yielding strength, ultimate strength and young's modulus have increased. It was observed that rates of critical strain energy and intensity of stress factors increase by reducing the temperature.

Dynamic strength of adhesive joint single lap to be precise was determined by Adamvalli [47]. The single lap joint was composed of titanium adherend and Araldite® 2014. The analysis was done at different temperatures 25°C to 100°C and at varying loading rates. The single lap joint was under the influence of dynamic loading. It was revealed by inspecting the joint that failure occur

was in adhesive layer. And the results of the study showed that at high temperatures strength reduced significantly whereas it was opposite for case of loading rate.

Nguyen and Bai [48] investigated adhesive joints of CFRP/steel double-strap joints exposed to mechanical and thermal loading. Loading levels was based on ultimate load at room temperature i.e. 80%, 50% and 20%. And the temperature was kept constant from 35 to 50°C for each load level. The joint strength and stiffness degradation as  $f_n$  (time and temperature) was shown by time-dependent behavior. It was also noted that for cyclic thermal loading almost 47% of recovery was noted in strength than that in constant temperature loading.

Rahmani and Choupani [49] investigated a composite adhesive joint of CFRP and aluminum. The purpose of their study to analyze the behavior of the joint at low temperatures i.e. -80°C to +22°C. Tensile testing was performed on the joint following by subject to temperature variation on the cracked joints. A FEM was designed to obtain a dimensionless stress intensity factor at low temperatures. Their results showed that the factors were improved by decreasing the temperature down to specific value after which the critical factors would decrease. That eventually led to reducing absorption of fracture energy capacity for the joint.

Ashcroft et al. [50] studied a double lap joints used in jet aircrafts and the joints were tested in fatigue through a temperature range and quasi-statically. Multi-directional MD and uni-directional UD CFRP were used as adherends for adhesive joints. Numerical study was conducted to study the stresses in the adhesive composite joints. The results showed that both strength of the joint and resistance to fatigue decreased as the temperature value is increased. In their study joints having MD CFRP adherends were stronger at low temperatures and joints having UD CFRP adherends were stronger at high temperatures. Their study proposed that the behavior they observed was due the fact that at low temperature, the strength of the adhesive joint is controlled by peak stresses whereas at high temperatures, the strength is of the joint is controlled by creep in the joint and determined by observing min. stresses in the adhesive joint. The finite element analysis supported this proposition.

Adamvalli and Parameswaran [47] Investigated the effect of temperature variation at elevated dynamic loading on the strength of the SLJ joint by using servo-hydraulic high-rate testing equipment. the results were shown by method of digital-image-correlation, and it depicts joint failure and strength. In the results it was observed that by increasing loading rate, bond strength

and shear strength was increased. Varying the temperature from  $-25^{\circ}\text{C}$  to  $50^{\circ}\text{C}$ , increase in average bond strength was observed. Whereas the strength of joint decreased by varying temperature from  $50^{\circ}\text{C}$  to  $100^{\circ}\text{C}$ . The results of the investigation also showed the behavior of the failure. At room temperature the failure of the joint is said to be due to steel/adhesive interface. At higher temperatures it was shifted to BFRP/adhesive interface.

It can be concluded from the literature in this section that the performance of the adhesive joint or composite adhesive joint is affected under different temperature conditions. From literature it is clear that mostly the strength of the composite or simple adhesive joint decrease with increase in temperature. The decrease in temperature has not similar affect as by increasing temperature. The literature shows that the stress intensity factors, which determined via FEM, are crucial. These factors increase to critical value and then decrease on further reducing the temperature.

## **2.7. Effect of Adding Nanoparticles into the Composite Adhesive Joint**

Farid Taheri [51] presented a summary that highlights the development of nanoparticles in this subject. Special emphasis on the papers that discusses the improving performance of adhesive bonded joints using nanoparticles. Articles with relevant numerical examination with particular emphasis on FEM is considered. Scarselli and Corcione [13] investigated single lap joints that were manufactured, test and simulated. Two types of adhesives were used: one was conventional adhesive i.e. joined with epoxy resin and the other was combination epoxy resin and nano graphite particles. Swelling method was used for dispersion graphene stacks that sonicated and expanded (EGS, 3%) in the matrix of epoxy. Their research shows superior mechanical properties in case with nano-graphite added with epoxy. This is evident by experimental characterization of the behavior of adhesive in terms of energy absorption and strength. Critical fracture energy and max. shear stress was obtained by using CZM.

Khashaba [52] worked on improving performance of adhesive bonded joint in composite structures by using Multiwalled Carbon-Nanotubes (MWCNTs) with Epocast 50-A1/946 epoxy. 40% improvement was observed compared to neat adhesive in a scarf adhesive joint SAJ. The study at elevated temperature was also conducted and results showed dramatic decrease in tensile strength moreover water abortion also affected tensile strength according to results 2 % decrease was observe in tensile strength compared to the dry one.



Khashaba [53] in another research investigated the dynamic analysis of an adhesive joint in which CFRP composite altered with Aluminum Oxide nanoparticles  $Al_2O_3$  under fatigue conditions at various temperatures. Hysteresis loop of stress-strain was used to analyze the dynamic parameters including storage modulus, potential and dissipated energy  $U_p$  and damping factor. The addition of the nanoparticles to scarf joint (SAJ) resulted in good results as it was observed that 4.8% increase in shear strength of the joint at room temperature and 24.5% rise at 50°C. The reduction in glass transition temperature at 50°C resulted in decrease in fatigue strength.

Andrea and Alessandro [54] investigated the effect of aluminum nanoparticles on the strength of epoxy. It was found out that fatigue life and shear strength increased remarkably by the presence of untreated alumina. Statistically, the shear strength increased by 60% and improved other properties. It was noted that inclusion of alumina particles improved mechanical properties of adhesive.

Sunil and Dharmendra [55] investigated the effect of nanoparticles on failure load of an adhesive joint. It was analyzed experimentally and numerically that the failure load increased by adding nanoparticles of alumina into the adhesive and used to form a single lap joint. The epoxy was reinforced with 23-47 nm alumina particles that were synthesized utilizing polymerization technique with 0.50 wt.%, 1.00 wt.%, 1.5wt.% and 2.00 wt.% of nanoparticles. It was noted in results that compared to neat adhesive joint; the failure load increased in case of nanoparticles added to the joint. Of all the cases, 1.5wt.% of alumina nanoparticle showed higher than 50% increase in shear strength of SLJ. 2D FEM modeling was constructed to compared it with experimental analysis and both the studies were in line with each other. Shear, von-Mises, and peel stress distribution were investigated to see the effects of reinforcement in the joint by finite element analysis.

Khashaba [56] investigated the including of different nanoparticle types into an epoxy adhesive. The purpose of this investigation was to compare the change induced by these infusions into the epoxy on mechanical characteristics of the adhesive joint. The nanoparticles include are MWCNTs,  $Al_2O_3$  and SiC with different weight %ages dispersed ultrasonically into epoxy Epocast 50-A1/946. To avoid damaging MWCNTs, the time of sonication and amplitude was decreased compared to SiC and  $Al_2O_3$  nanoparticles. In plane shear and standard tests were conducted on neat and twelve nanocomposite joints. The experimentation showed that MWCNTs (0.5wt.%),

SiC (1.5wt.%) and Al<sub>2</sub>O<sub>3</sub> (1.5wt.%) exhibits greater improvements in properties of tensile when compared to other weight percentages of nanoparticle materials. MWCNTs, SiC and Al<sub>2</sub>O<sub>3</sub> improved the shear strength by 5.5%, 4.9%, and 6.3% respectively. MWCNTs, SiC and Al<sub>2</sub>O<sub>3</sub> improved the shear moduli by 10.3%, 16.0%, and 8.1% respectively.

Salom and Prolongo [57] investigated the effect of graphene nanoplatelets (type and content) on the thermo – mechanical and properties of graphene epoxy nanocomposite. All nanocomposites showed higher modulus than pure epoxy thermoset resin. The storage modulus increase was higher in rubber state than in glass state. Nanocomposites were fragile, showing less tensile strength than pure epoxy thermoset resins due to the aggregation of graphene nanoplates. Epoxy-GNP<sub>NH2</sub> nanocomposites are lower Reduced tensile strength and reduced fragility. Epoxy-graphene adhesives have less overlap shear Strength as a pure epoxy adhesive. Increased CLT content led to lower lap shear strength. Two types of graphene used: functionalized and unfunctionalized. Amine groups were contained in functionalized graphene GNP<sub>NH2</sub>.

## **Chapter 3: Finite Element Modeling**

### **3.1. Introduction**

A Finite Element Analysis FEA was performed for the problem using Finite Element Modeling tool Abaqus CAE developed by Dassault Systems. A 3D model of Composite Fiber Reinforce Polymer CFRP and Aluminum 5083 was modeled in Abaqus standard module. The adhesive representing Epocast 50-A1 Resin/ Hardener 946 was also employed in the same module. Elastic and plastic material properties were taken from reference [53]. The focus of the study was to generate two cases of the problem one analyzing the single lap joint with neat adhesive that is the epoxy without any filler concentration. Second case was simulating the single lap joint with mixture of epoxy and Aluminum Oxide  $Al_2O_3$  nanoparticles. The influence of temperature at 25°C and 50°C on the behavior of composite adhesive joint was also a major focus presented this study.

### **3.2. Initial Geometry Configuration**

The geometry of the SLJ is shown in the figure 3.1. The dimensions of CFRP, Aluminum and adhesive region was taken from an experimental study [58]. The adherends have two different materials. One adherends is modelled as aluminum 5083-H116 while the other adherend is modelled as Composite Fiber Reinforce Polymer CFRP. The CFRP is modelled as bi-directional material in which the layers are stacked perpendicular to each other that is 0° and 90°. Both Aluminum and CFRP have same length of 101.6 mm and width of 25mm whereas Aluminum has thickness of 1.51mm and Composite adherend has thickness of 2.15mm.

In other words, the dimensions of Aluminum are 101.6 x 25 x 1.51 mm and composite adherend has 101.6 x 25 x 2.15 mm. These dimensions were taken from an experimental study focused on analyzing strength of composite adhesive joint by varying temperature and cork particles weightage. The dimensions for adhesive region were also taken from that research which were 25.4 x 25 x 0.1 mm.

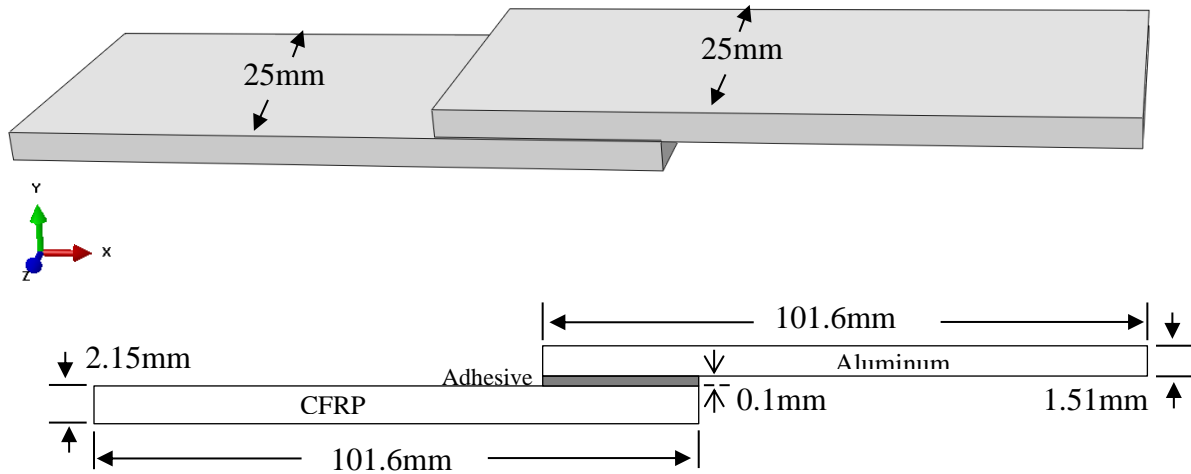


Figure 3.1: Geometry of Single Lap Joint (Not to Scale)

The model for aluminum and composite adherend was linear elastic. That means that the stress-strain behavior of these adherend was considered to be elastic only. Whereas the adhesive behavior was considered as elastic and plastic at room temperature 25°C, 50°C and 75°C. The material properties of the adherends and adhesives used are listed in the table below [56].

Material Property	Aluminum 5083	Neat/Epoxy	1.5wt% Al <sub>2</sub> O <sub>3</sub> /Epoxy
Elastic Modulus (E) (GPa)	70	3.432	3.676
Poisson Ratio ( $\nu$ )	0.33	0.32	0.314
Shear Modulus G (GPa)	26.4	1.45	1.57
Tensile Strength (MPa)	317	75.53	75.88
Shear Strength (MPa)	190	50.71	53.91

Table 3-1: Material Properties of Al 5083, Neat adhesive, and adhesive with Al<sub>2</sub>O<sub>3</sub> nano particles [56]

Material Property	E <sub>1</sub> (GPa)	E <sub>2</sub> =E <sub>3</sub> (GPa)	$\nu_{12}=\nu_{13}$	$\nu_{23}$	G <sub>12</sub> =G <sub>13</sub> (GPa)	G <sub>23</sub> (GPa)
Elastic Properties	135	8.8	0.33	0.45	4.5	4.0

Table 3-2: Material Properties of T300/QY8911 CFRP Composite Lamina [59]

The composite fiber reinforced plastic CFRP was constructed bi-directional layer method. The bi-directional signifies the structure or the layer applied while making the CFRP manually in a lab. The piles are perpendicular to each other which means one layer is applied at 0° and other is at 90°. Following his method, the layers are staked on each other the total count of the layers are 7. Whereas each ply thickness was measured to 0.307143 mm. the overall length, width and thickness is 101.6 x 25 x 2.15.

### 3.3. Loading and Boundary Conditions

The Boundary and loading conditions for the application of finite element analysis on the single lap composite adhesive joint is shown in the figure 3.2. Two types of boundary conditions were used on the SLJ. One was encastre boundary condition used in the left adherend/CFRP fixing the edge of the CFRP. Second was displacement boundary condition applied on the right adherend/aluminum. Tensile loading using displacement loading of 0.3 mm was applied to the right adherend of the SLJ. The SLJ was only allowed one degree of freedom that is x-direction, and it was fixed in y-direction to prevent any vertical movement. This was done by applying roller support on right adherend as shown in the figure below. A tie constraint was used between contact surfaces of adhesive and adherends.

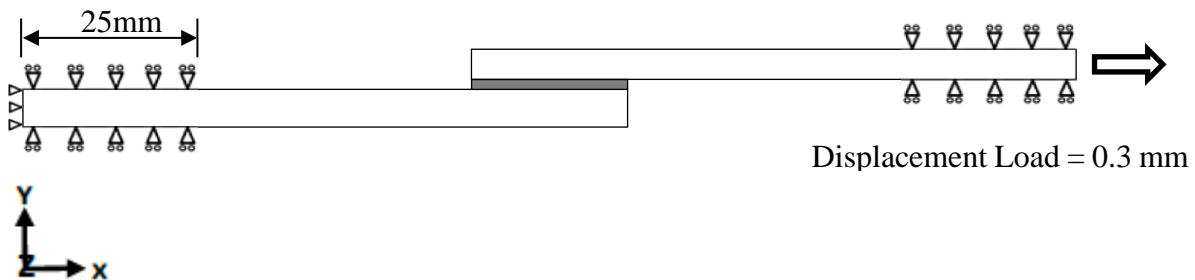


Figure 3.2: Boundary and Loading Conditions of Single Lap Joint SLJ (Not to Scale)

### 3.4. Meshing Methodology and Element Formulation

The meshing of the model was a challenging task because of the thin adhesive layer compared to the CFRP and aluminum adherends. In tensile loading the bending of SLJ is an important factor to consider when applying mesh more importantly in single lap joints where there is eccentric

loading. The mesh can be considered as well meshed if it is able to represent deformed and undeformed shape of the SLJ effectively.

Generally, two types of methodologies are there for meshing an adhesive joint. First method is generating a variable mesh that transit form coarse mesh to fine mesh at a particular region of interest. For this method the SLJ is divided or partitioned into several regions which allows to seed the regions separately and provide variable seeds sized along the edges of the regions. In second method the mesh is applied to each part separately. That means the region of interest can have fine mesh like the adhesive and the regions that are not of interest comparatively can be mesh as coarse such the CFRP adherend and Aluminium adherend. Hence coarse mesh can be applied to the adherends, and fine mesh is needed in the adhesive. There is more pre-processing involved in the first method as the part or the model is partitioned in regions that can seed individually and separately, thus required more pre-processing time than the second method. In this research the second method is employed on the SLJ parts. The reason behind employing the second method is due to the fact that the CFRP required only one element in the stacking direction of the piles which the thickness of the adherend.

All parts of the single lap joint were meshed by “structured mesh” methodology. This method uses predetermined pattern and shape of element unlike “free mesh”. The CFRP adherend is given structured mesh with one element along thickness. The aluminium adherend has two elements along thickness while the adhesive layer has four elements along thickness. All parts are mesh as structured mesh. From the figure 3.5 the parts are meshed with elements of rectangular shape that is structured mesh by meshing module. The region of interest is meshed fine whereas the other regions are coarse mesh.

The global mesh size for the CFRP and Aluminium adherends is 1mm. Whereas local seeding method was used for the adhesive containing four elements in thickness direction. All the elements were of uniform size. Approximately 300 elements on each edge of the adhesive layer were set. The total number of elements in the adhesive layers are 3,71,526.

### **3.5. Type of Mesh Elements**

Based on the response to tensile loading, the mesh element type was considered for the adhesive joint. The single lap joint experience bending in the application of tensile loading due to the eccentricity of the load applied.

Linear 8-node brick element with reduced integration (C3D8R) was used for the aluminum adherend and adhesive region. Whereas quadrilateral continuum shell element (SC8R) was used for carbon fiber reinforced plastic CFRP. The reason for choosing different type of element is due to CFRP layers can only be modeled solid shell model. There is specific family of element which continuum shell for the meshing CFRP adherend. The figure 3.5 clearly shows the meshing of the parts of SLJ.

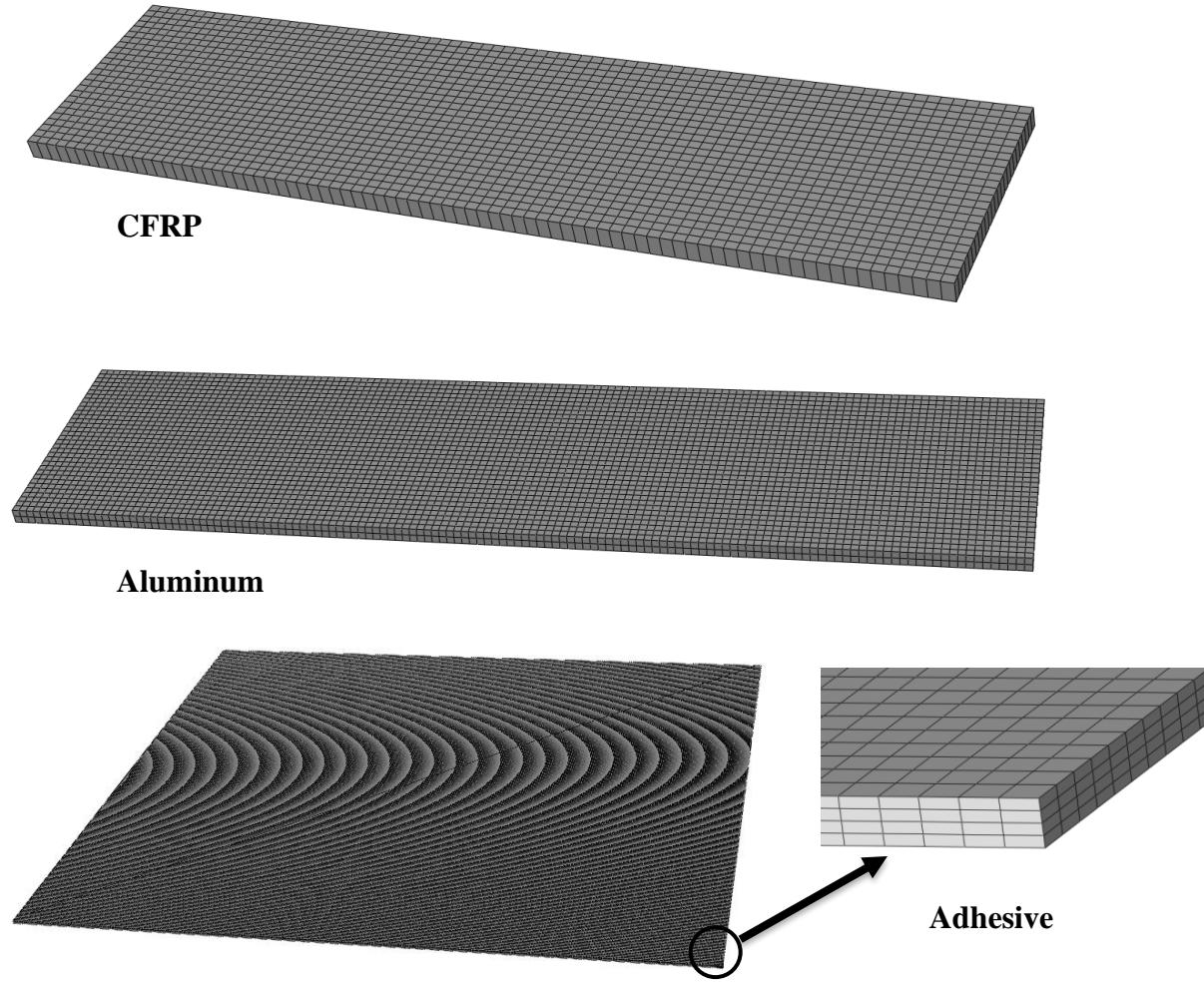


Figure 3.3: Partwise SLJ Meshing



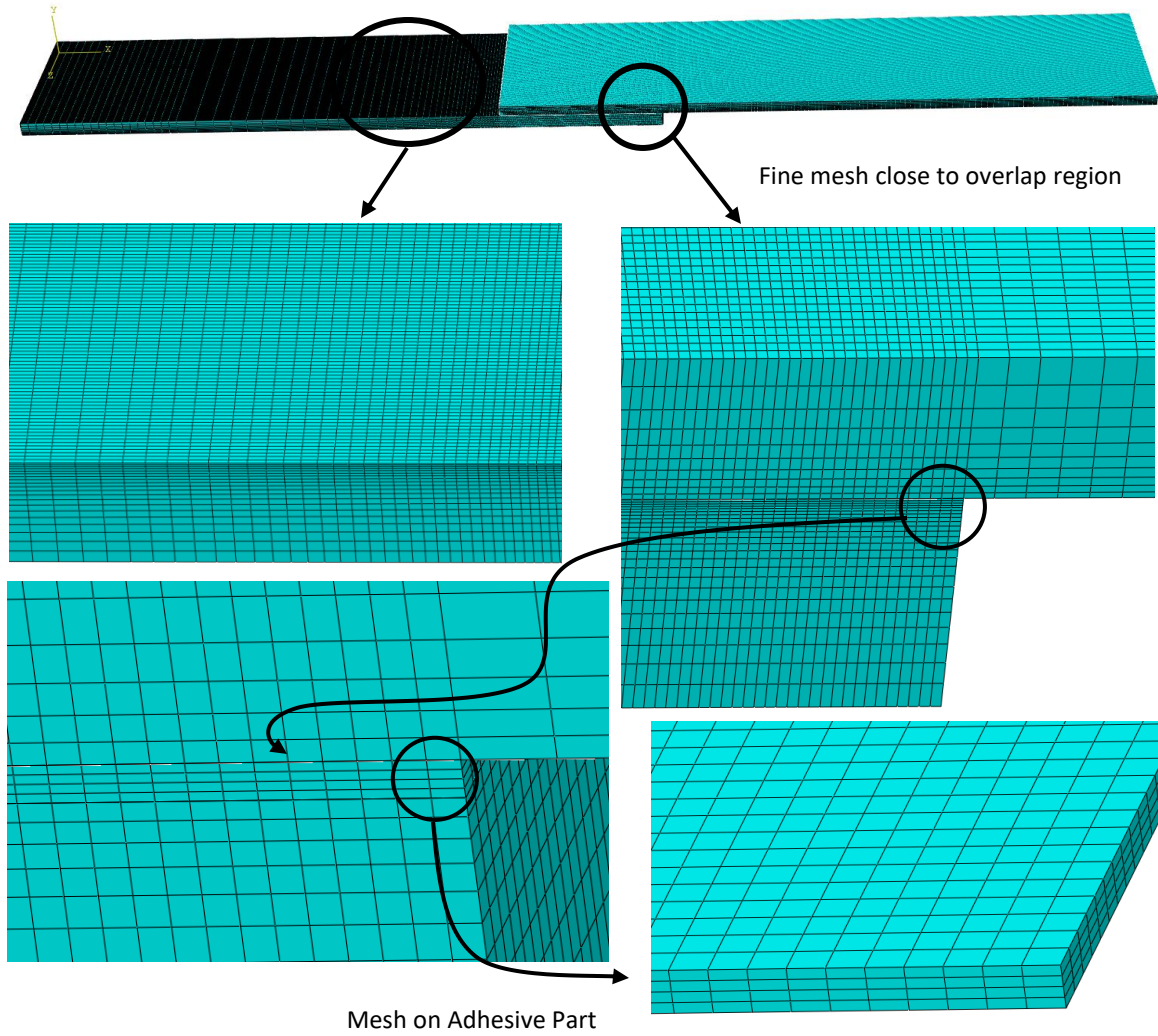


Figure 3.4: Detailed Meshing of SLJ

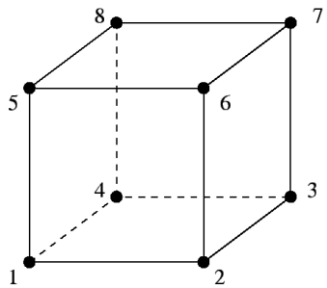


Figure 3.5: C3D8R (An 8-node linear brick, 3D Stress Element)

### 3.6. Validation of Finite Element Model

The finite element model of the adhesive joint, the results of a Single Lap Joint was compared with a data that was published in [23]. Taking the concept of 2D stress analysis from that work and

translating it to the current work. The fundamentals of 2D and 3D stress analysis are same despite in 3D, there is a third axis that gets involved. Moreover, there were no literature found like or close to the work that is under discussion in this document. That is why initially the study was started with a 2D problem and later on converted to a 3D problem. In ref. [23] peel stress study was conducted on the single lap joint shown in the following figure.

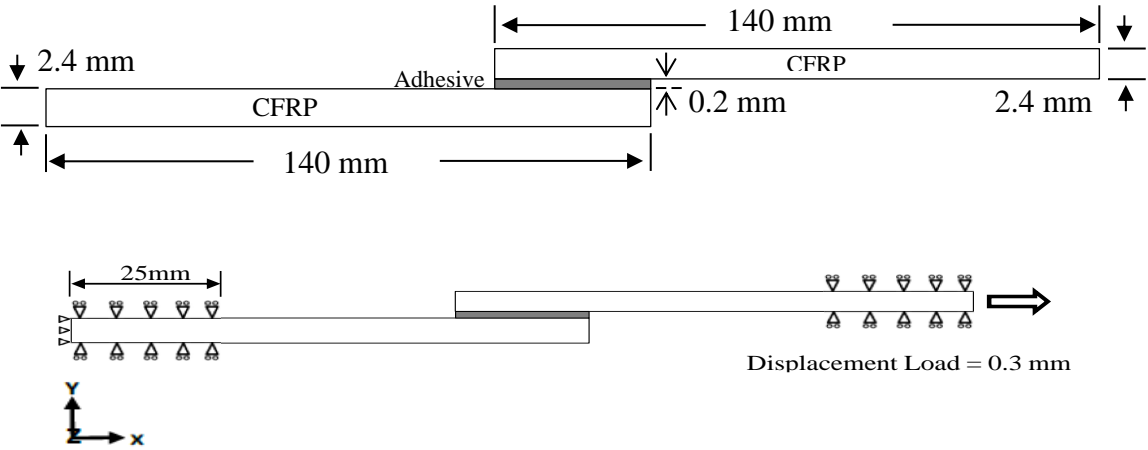


Figure 3.6: Single Lap joint with composite adherends used for validation work

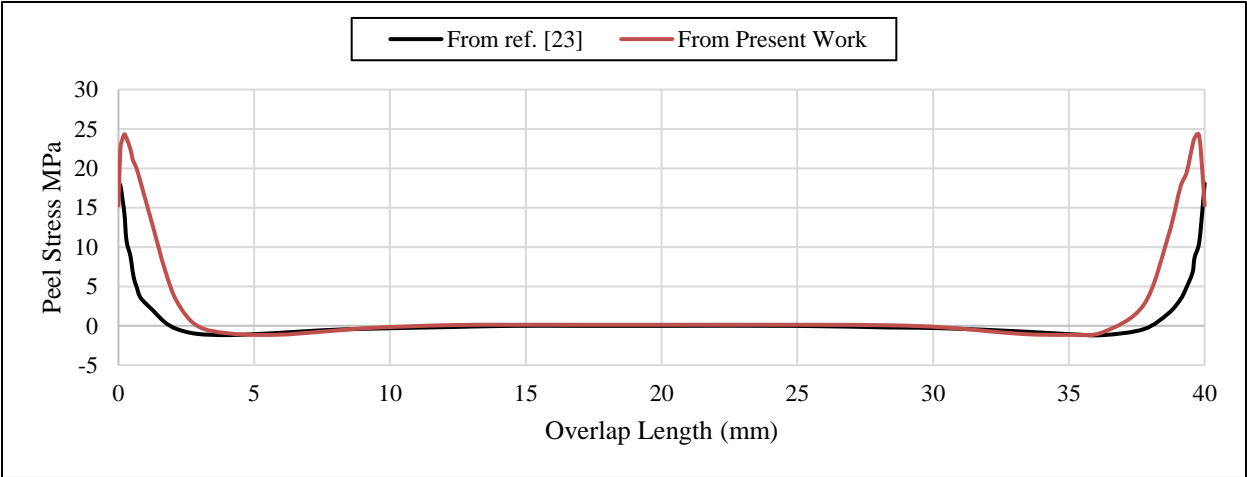


Figure 3.7: Comparison of Peel Stress in the middle of adhesive layer of SLJ between reference and present study.

The figure 3.7 shows the comparison between the reference study and present study carried on the model geometry in the figure 3.6. The present work shows higher peel stress inside adhesive whereas the ref. work shows it at the edge of adhesive. The difference between the studies at the ends of the adhesive may be due the application of traction separation law which is not applied in

the present work. The cohesive zone model was also not applied in present work. Other than that, there is good correlation between them. Moreover, the trend is identical in this phenomenon which indicated that analyzing the single lap joint, the ends of the joint gets high stresses and are more vulnerable to failure.

## Chapter 4: Results and Discussion

In this chapter result of the present work is discussed with graphical data that was acquired during the FEM analysis. The cases that are focus of this research are: 1) SLJ with Neat adhesive that is the adhesive is pure Epocast 50-A1 Resin/ Hardener 946. 2) SLJ with Alumina nanoparticles added to the neat adhesive. the SLJ is subjected to different temperature including  $25^{\circ}\text{C}$ ,  $50^{\circ}\text{C}$  and  $75^{\circ}\text{C}$ . The effect of nanoparticles of the SLJ at geometrical locations is the prime objective of this research. The results are focused on the stresses such as peel and shear the occur in adhesive layer during loading of SLJ at four specific locations. These locations are; the middle of long edge face (along length of adhesive), the top face middle (between adhesive layer and aluminum adherend), the middle plane of adhesive layer, and the middle of short edge face (along the width) of adhesive layer. Paths were drawn to at these locations to get the required results. The cases are discussed individually, and a comparative discussion is given separately.

### 4.1. Neat Adhesive SLJ

The single lap joint SLJ having neat adhesive was subjected to tensile loading by applying displacement of 0.3 mm. Due to eccentricity, The SLJ is experience bending which cause peel stresses and shear stresses are cause by the tensile loading. In this research, peel stress and shear stress in the SLJ at four different locations. These are the middle of long edge face (along length of adhesive), the top face middle (between adhesive layer and aluminum adherend), the middle plane of adhesive layer, and the middle of short edge face (along the width) of adhesive layer. The SLJ is also analyzed at different temperatures including  $25^{\circ}\text{C}$ ,  $50^{\circ}\text{C}$  and  $75^{\circ}\text{C}$ . In the following text peel stress and shear stress distribution over the overlap region of the joint is discussed at the location separately.

#### 4.1.1. At the Middle of Top Face (Interface)

The location of the data collection is given in the figure 4.1. At the interface of adhesive and aluminum, peel stress shows greater variation along the length. But eventually reaches zero stress. The graph can be seen to go down less than zero which indicates that the compressive stress. The variation is high for adhesive at  $25^{\circ}\text{C}$  compared to adhesive at  $50^{\circ}\text{C}$  and  $75^{\circ}\text{C}$ . This is due to stiffness of the adhesive at lower temperature and as the temperature is increased the stiffness and

elastic modulus of adhesive was decreased. From the figure 4.2, it is noticed that there is high peel stress at the edges of the adhesive. due to bending the material is peeling from edges that shows higher stress at the ends of adhesive. if the failure of the joint is considered, the crack initiation is more likely to start from the edges. From the results in the graph, 39% decrease in the peel stress was recorded by increasing the temperature from 25°C to 50°C and 51% decrease in the peel stress by increasing the temperature from 50°C to 75°C.

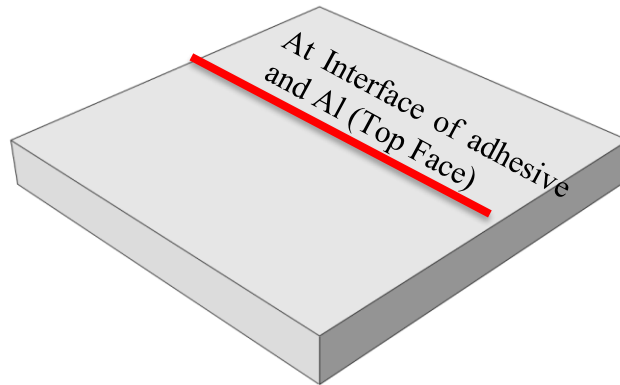


Figure 4.1: Path drawn at interface of Neat Adhesive and Aluminum for Peel Stress and Shear Stress Results

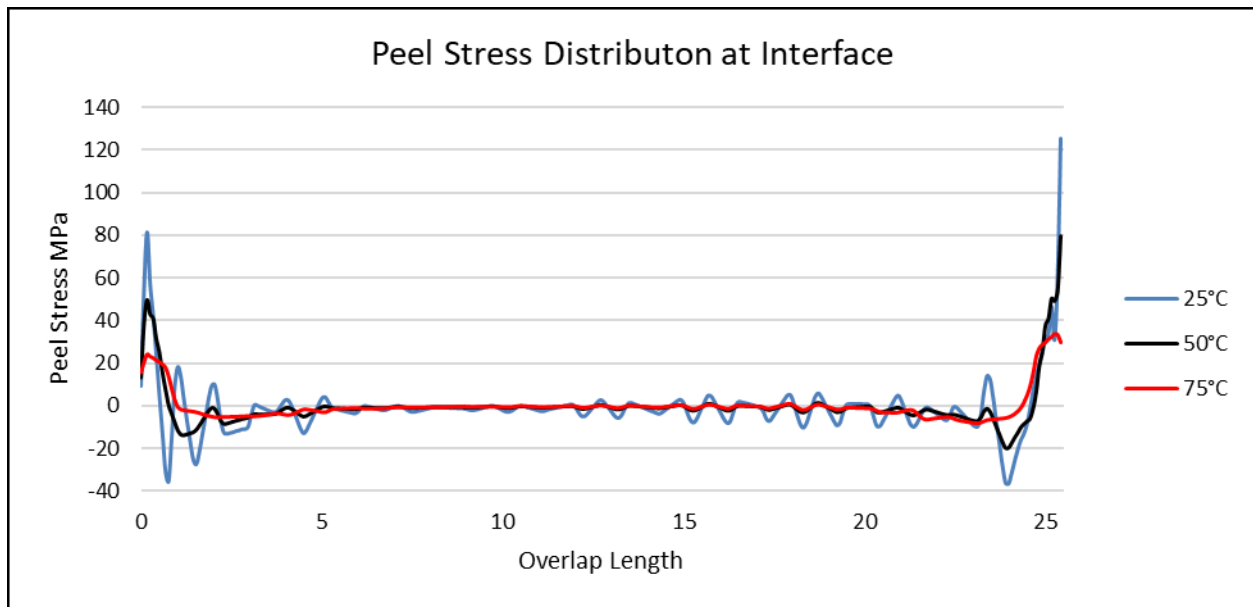


Figure 4.2: Peel Stress distribution at the interface of the overlap region of Neat-SLJ at different temperatures

The shear stress is in the SLJ occurred due the tensile loading. This type of stress plays important role in determining the strength of an adhesive joint. For that purpose, in this study the effect of

temperature on shear stress at different locations at Adhesive region is analyzed, for instance at the interface for this case. It is shown that at room temperature, SLJ experience more shear stress than at 50°C and 75°C. Due low elastic and shear modulus at higher temperature, the max. shear stress recorded as 32MPa compared to 100MPa at 50°C. As the temperature increases from 25C to 50C, 45% decrease in peak shear stress is recorded. Whereas 33% decrease in peak shear stress is shown for increase in temperature from 50C to 75C.

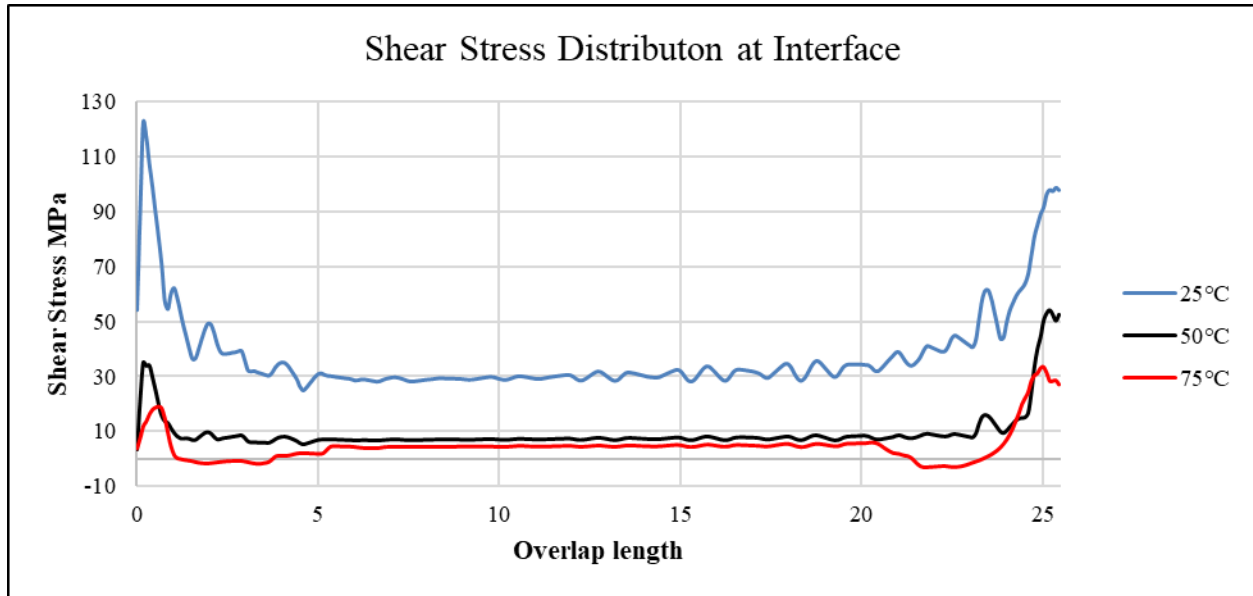


Figure 4.3: Shear Stress distribution at interface the overlap region of Neat-SLJ at different temperatures

Considering the physics of the joint it evident from the figure 4.2 that the failure is more likely to start from the point that is 0.7 mm inwards from the edge. Peel stress has more role in initiating the crack in the joint. That is why studying this stress is important and by looking at the figure 4.2, the crack will initiate from both edges of the joint and propagate towards the center of adhesive. Peel stress is high at 25C than at 50C and 75C. The more plausible reason is due to the resistance to the change in deformation in tensile loading. At room temperature this resistance is high compared to high temperatures. At high temperature the adhesive elastic modulus is decreased which allow more yielding to the applied load leading to low peel stress at that temperature. This phenomenon can be seen at the peel stress distribution figure, at 50C there is 39% decrease in peak peel stress compared to 25C. Which gives the idea that the failure load for the joint at 50C will less than at 25C. Moreover, the neat adhesive will sustain the peak load for longer period of time

than adhesive with nano-fillers, which will be discussed later. This argument can be justified using the ref. [56] in which through experimentation it is proven that adding  $\text{Al}_2\text{O}_3$  nano particles to Epocast 50-A1 adhesive makes it more stiff. But it will also help to withstand more load than neat adhesive.

#### 4.1.2. At middle plane of adhesive

The path at the middle plane of the adhesive is shown in the figure below. It can be noted that compared to peel stress at top face (interface), at this location peel stress is lower. According to the results the peak peel loads are: 74.4 MPa, 48.6 MPa, 24.6 MPa for 25°C, 50°C, and 75°C respectively. Increasing temperature from 25°C to 50°C 35% decrease in peel stress is recorded. Whereas increasing temperature from 50°C to 75°C 49% decrease in peel stress is recorded. It is similar for shear stress as well, the peak shear stress in adhesive of the joints is appeared to be 115.34 MPa, 38.5MPa, 18 MPa for 25°C, 50°C, and 75°C temperatures respectively. When the temperature is increased for 25°C to 50°C, 67% decrease in shear stress is shown which is lower than that appeared at the interface. Similarly, 53% decrease is recorded for temperature increase from 50°C to 75°C.

The mechanics of this case is similar to the case discussed above with slight difference in peak peel stress which is lower in this case. The logical reason is due to the location where the peel stress is recorded. The interface is prime location where adhesive will experience more peeling than at the middle plane. The other mechanics is similar to the above case.

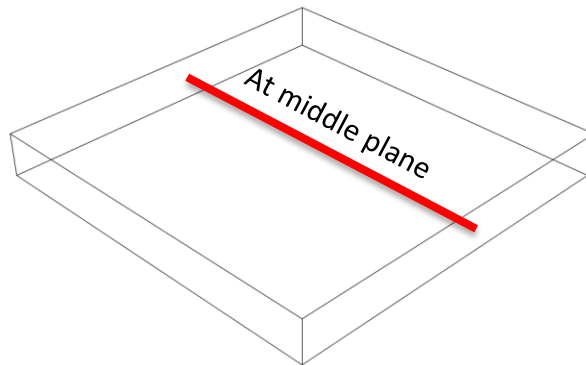


Figure 4.4: Path drawn at middle plane of Adhesive for peel stress and shear stress results

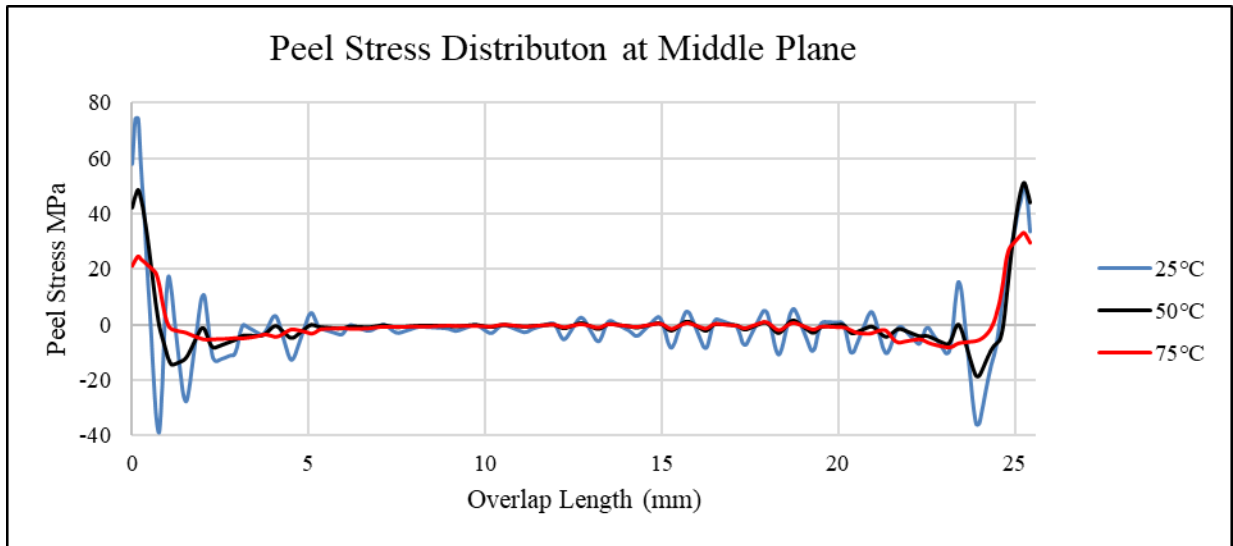


Figure 4.5: Peel Stress distribution at middle plane of adhesive at different temperatures

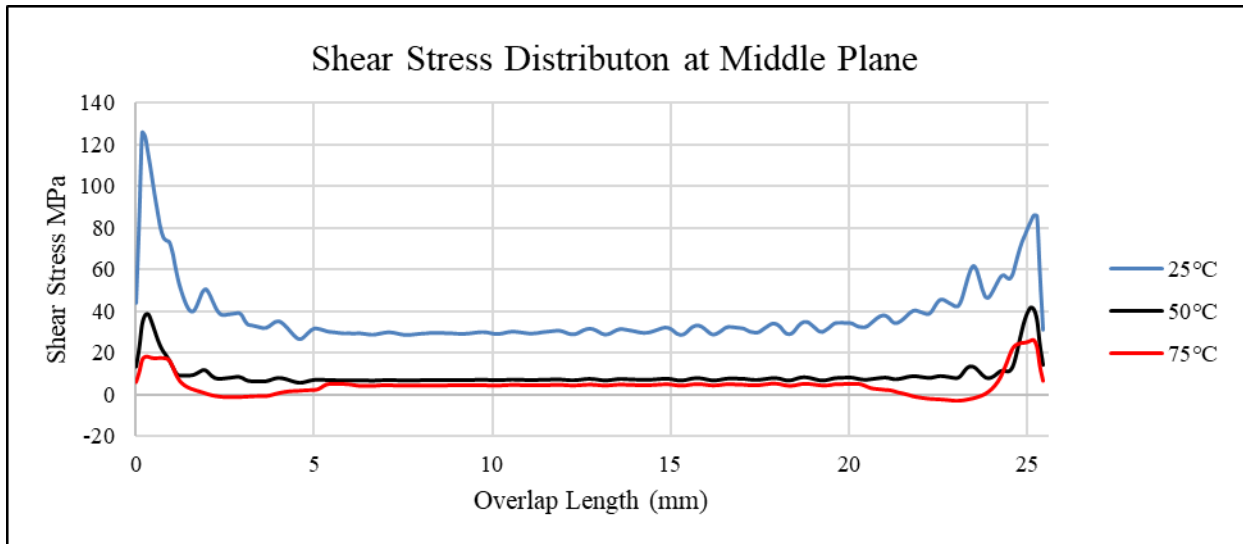


Figure 4.6: Shear Stress distribution at middle plane of adhesive at different temperatures

#### 4.1.3. At the longer edge of adhesive (along length)

Results for peel stress and shear stress at the middle of longer side of the adhesive is given below. The peak peel stress and shear stress is low at this location compared to the previous locations. The peak peel stresses are 62.6 MPa, 34.3 MPa, and 10.5 MPa at 25°C, 50°C, and 75°C respectively. Whereas the peak shear stresses are 110.063 MPa, 25.6 MPa, and 4.1 MPa at 25°C, 50°C, and 75°C temperature respectively. The peeling of adhesive is occurring at the end of the



adhesive region and as the stress goes down to the middle of the region it approaches zero stress or minimum.

The mechanics for the joint at this location is not quite different with above cases but there are some differences. Highlighting the main difference which is the drop in Peak peel stress and the behavior of neat adhesive at higher temperature. The peak peel stress is dropped to 62 MPa at room temperature. Moreover, from the figure 4.8 the peak stress is 0.7 mm inside the adhesive from the edge at 25C but the peak peel stress at 50C and 75C it is at the edge. As the temperature decreased the stiffness in the adhesive is decreased drastically.

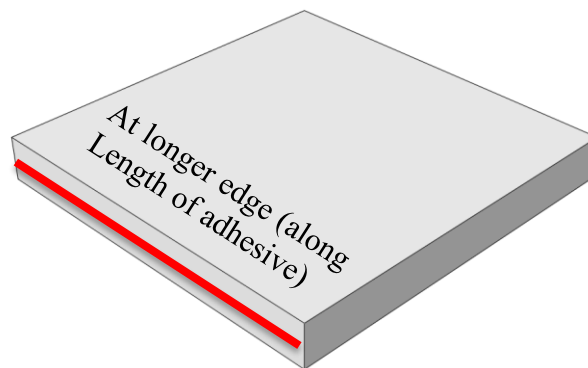


Figure 4.7: Path drawn at longer edge of Adhesive for peel stress and shear stress results

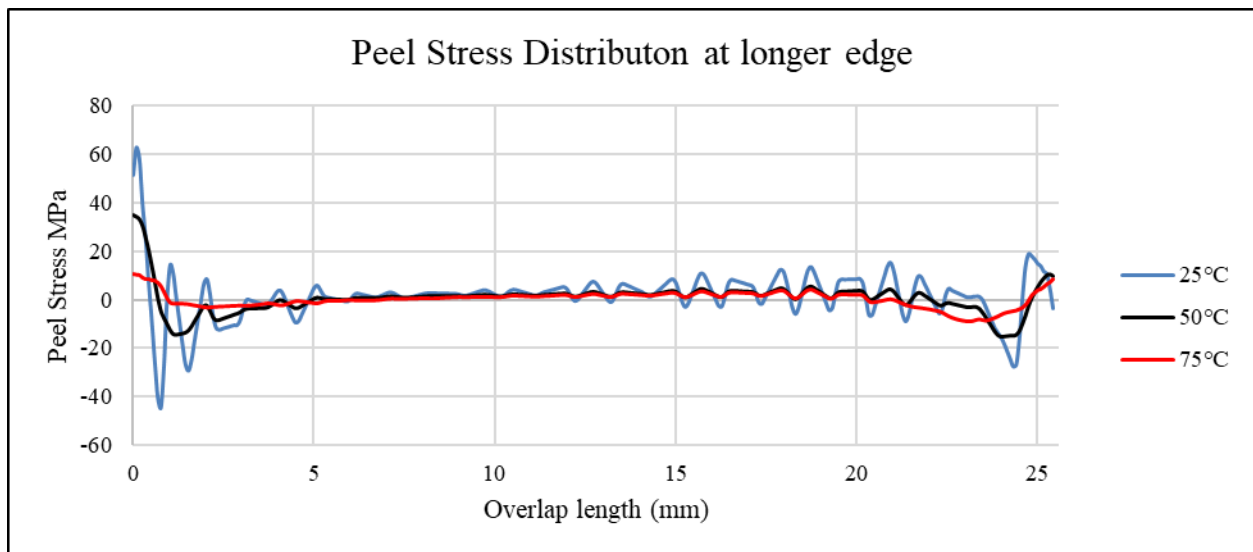


Figure 4.8: Peel Stress distribution at Length Side of adhesive at different temperatures

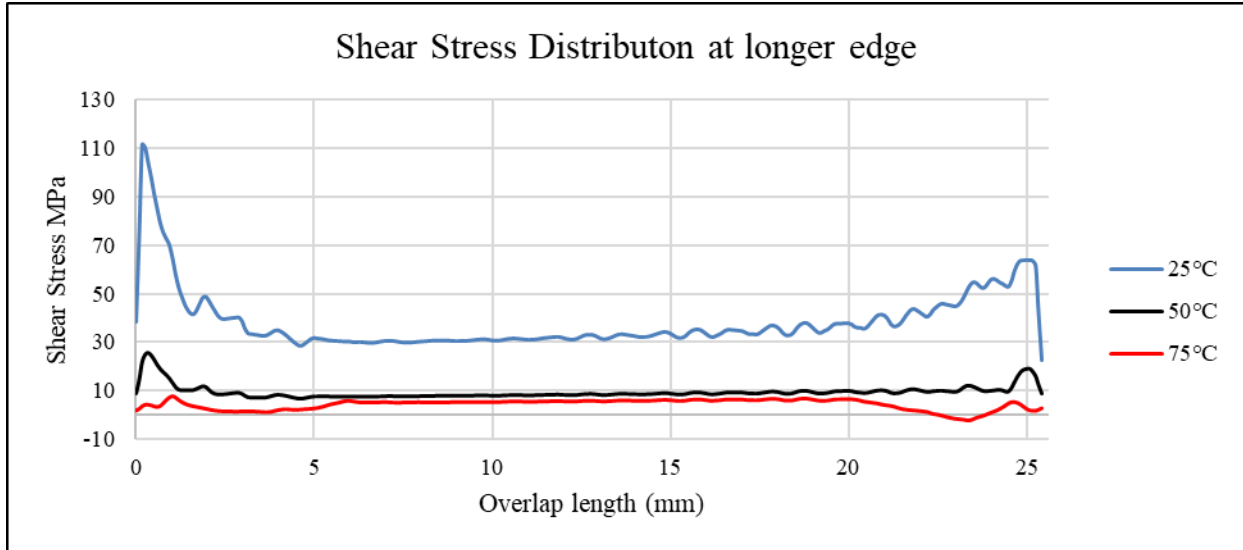


Figure 4.9: Shear Stress distribution at Length Side of adhesive at different temperatures

#### 4.1.4. At the Shorter Edge of Adhesive (along width)

The results of peel stresses and shear stresses at this location is completely different from the previous cases. Both peel and shear stresses low at edges and climb to higher value as we move towards the center. Peak values for Peel Stress are 36 MPa, 44 MPa and 30 MPa at 25°C, 50°C, and 75°C respectively with percentage increase of 22% in the peak value of peel stress for temperature increase from 25°C to 50°C. Whereas the value decreased by 30% at 75°C. The peak values for Shear Stresses are 31 MPa, 14 MPa and 6.6 MPa at 25°C, 50°C, and 75°C respectively. The peak value decrease as the temperature increased. 55% for 25°C to 50°C and 53% for 50°C to 75°C.

Considering the mechanics of the joint for this case, it is same as other cases in terms of decreasing trend with increase in temperature. At this location as the tensile load is applied, the material tries to move towards the center of the adhesive. The adhesive resists more at the center to deform than at the edges. It is because there is no material attached to the adhesive at the edges. Which results in lower peel stress at the edges and higher peel stress at the middle.

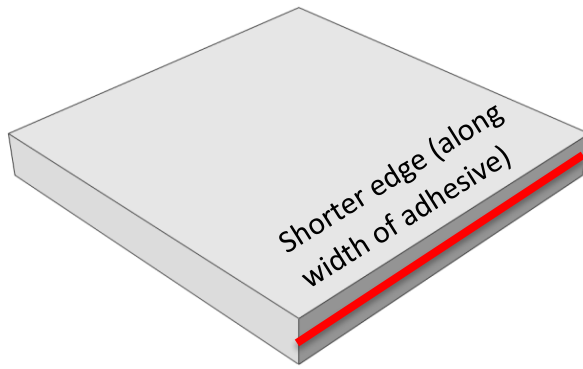


Figure 4.10: Path drawn at Width Side of Adhesive for peel stress and shear stress results

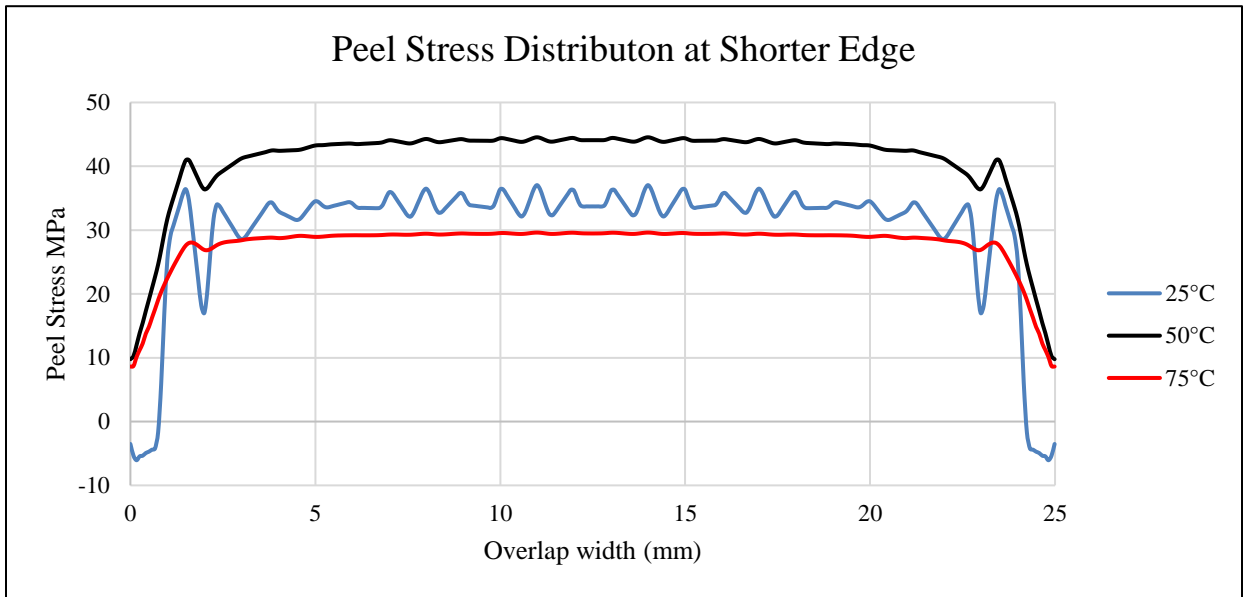


Figure 4.11: Peel Stress distribution at Width Side of adhesive at different temperatures

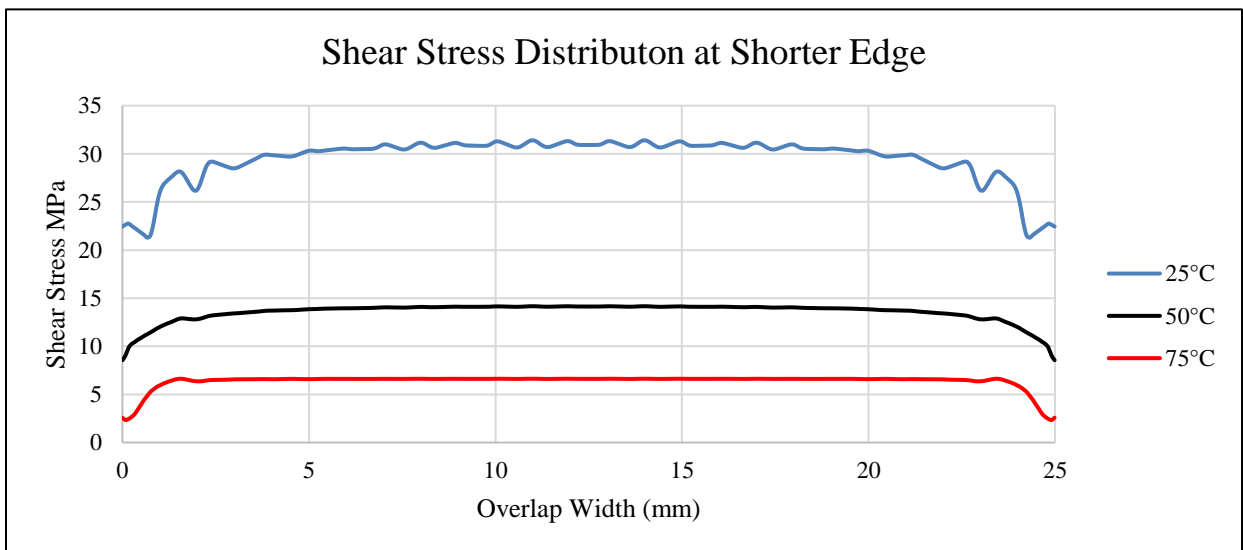


Figure 4.12: Shear Stress distribution at Width Side of adhesive at different temperatures

## **4.2. Adhesive Joint with Alumina Oxide ( $\text{Al}_2\text{O}_3$ ) Nanoparticles**

The single lap joint SLJ having alumina oxide nano  $\text{Al}_2\text{O}_3$  particles added to the adhesive was subjected to tensile loading by applying displacement of 0.3 mm. Due to eccentricity, The SLJ is experience bending which cause peel stresses and shear stresses are cause by the tensile loading. In this research, peel stress and shear stress in the SLJ at four different locations. These are the middle of long edge face (along length of adhesive), the top face middle (between adhesive layer and aluminum adherend), the middle plane of adhesive layer, and the middle of shorter edge face (along the width) of adhesive layer. The SLJ is also analyzed at different temperatures including 25°C, 50°C and 75°C. In the following text peel stress and shear stress distribution over the overlap region of the joint is discussed at the location separately.

### **4.2.1. At the Top Face of adhesive (interface)**

The stresses at this location is shown in figure 4.13. The red line shows the path that was drawn in the middle of adhesive and at the interface of adhesive and aluminum adherend. At the interface of adhesive and aluminum, peel stress shows greater variation near the ends of the adhesive. But approach zero stress at the middle region. The graph can be seen to go down less than zero which indicates that the compressive stress near the edges or ends of the region of adhesive. The variation is high for adhesive at 25°C compared to adhesive at 50°C and 75°C. This is due to high stiffness and elastic modulus of the adhesive material at lower temperature and as the temperature is increased the stiffness and elastic modulus of the adhesive material has decreased. From the figure 4.14, it is noticed that there is high peel stress at the edges of the adhesive. Due to bending the material is peeling starts from edges which is why the figure shows higher stress at the ends of adhesive. If the failure of the joint is considered, the crack initiation is more likely to start from the edges. From the graph, 33% decrease in the peel stress was recorded by increasing the temperature from 25°C to 50°C and 49% decrease in the peel stress by increasing the temperature from 50°C to 75°C.

For Shear Stress distribution, it is shown that at room temperature that SLJ experience more shear stress then at 50°C and 75°C. Due low elastic and shear modulus at higher temperature, the max. shear stress recorded as 35MPa at 75°C compared to 100MPa at 25°C. As the temperature

increases from 25°C to 50°C, 37% decrease in peak shear stress is recorded. Whereas 41% decrease in peak shear stress is shown for increase in temperature from 50°C to 75°C.

The mechanics of the joint involving adhesive with Al<sub>2</sub>O<sub>3</sub> nano fillers shows that adding the alumina particles improves material properties of the adhesive. Phenomenon of the joint stretching is similar to the first case of neat adhesive but there are some changes like difference between peak peel stress and Peel stress along the ends of the adhesive.

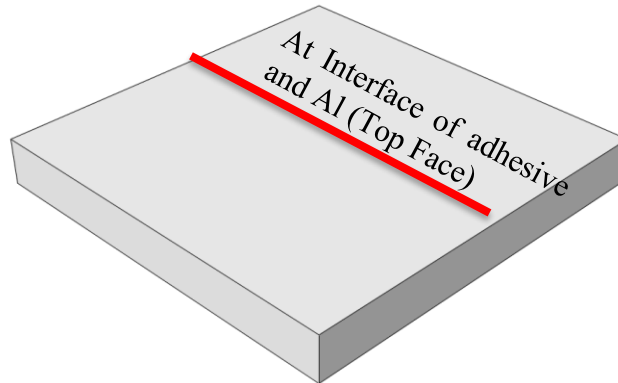


Figure 4.13: Path drawn at interface of Al<sub>2</sub>O<sub>3</sub> nano particle Adhesive and Aluminum for Peel Stress and Shear Stress Results

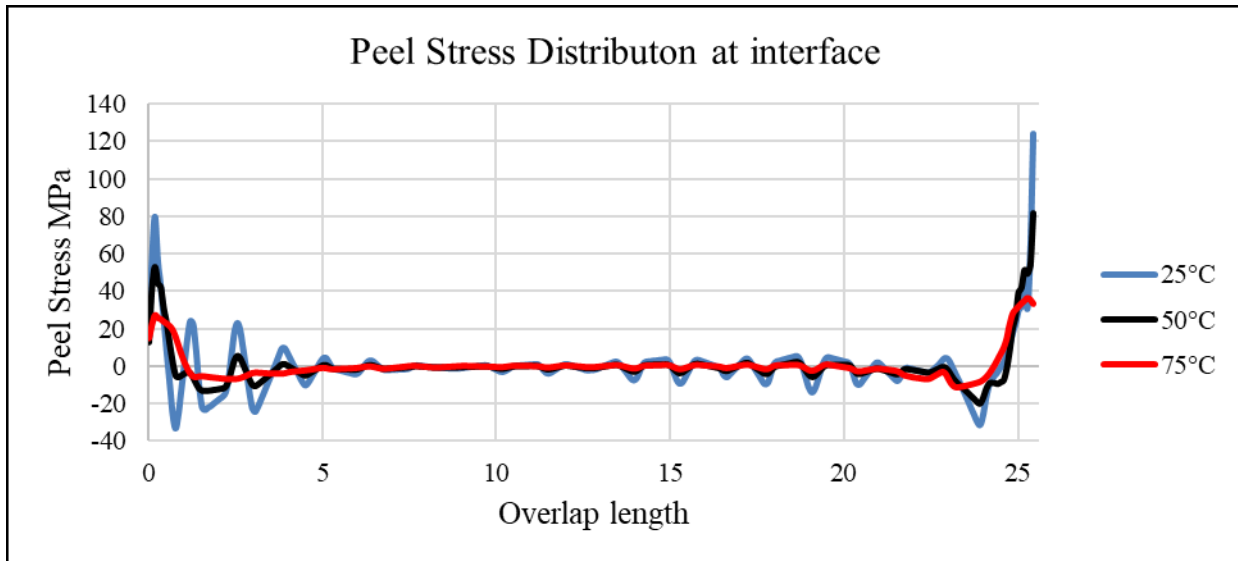


Figure 4.14: Peel Stress distribution at the interface of the overlap region of Al<sub>2</sub>O<sub>3</sub> nano particle-SLJ at different temperatures

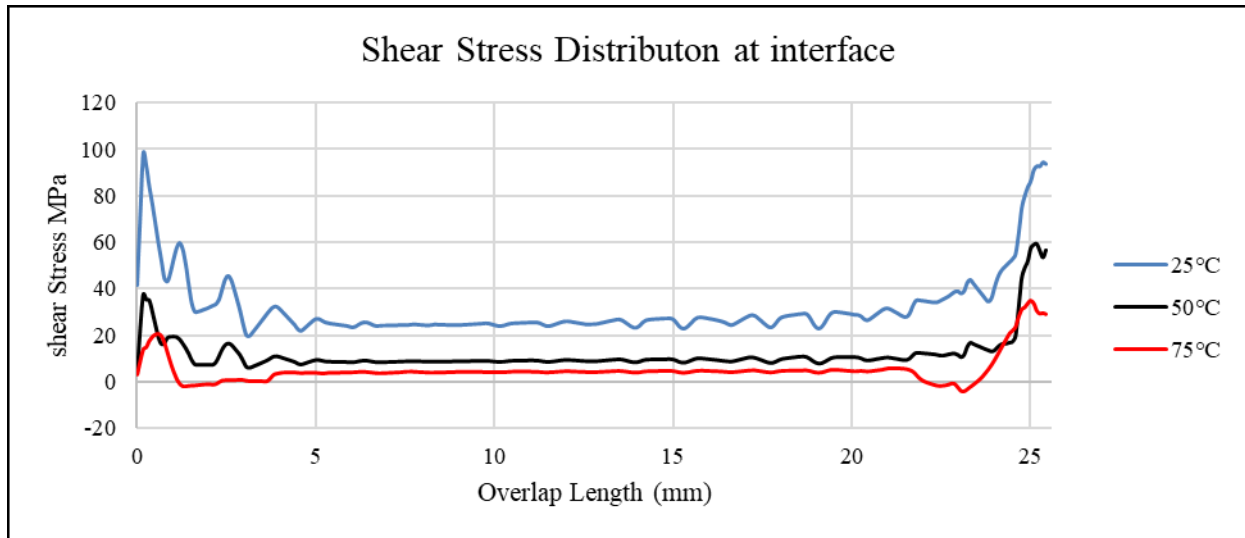


Figure 4.15: Shear Stress distribution at interface the overlap region of Al<sub>2</sub>O<sub>3</sub> nano particle-SLJ at different temperatures

#### 4.2.2. At middle plane of adhesive

The path drawn at the middle plane of adhesive as shown in the figure 4.16. It can be noted that compared to peel stress at interface, at this location peel stress is lower. According to the results the peak peel loads are: 72 MPa, 51 MPa, 27 MPa for 25°C, 50°C, and 75°C temperatures respectively. Increasing temperature from 25°C to 50°C 29% decrease in peel stress is recorded. Whereas Increasing temperature from 50°C to 75°C 47% decrease in peel stress is recorded. It is similar for shear stress as well, the peak shear stress in adhesive of the joints is appeared to be 81 MPa, 45 MPa, 26 MPa for 25°C, 50°C, and 75°C respectively. When the temperature is increased from 25°C to 50°C, 44% decrease in shear stress is shown which is lower than that appeared at the interface. Similarly, 42% decrease is recorded for temperature increase from 50°C to 75°C.

The mechanics of this case is similar to the case discussed above with a slight difference in peak peel stress which is lower in this case. The logical reason is due to the location where the peel stress is recorded. The interface is the prime location where adhesive will experience more peeling than at the middle plane. The other mechanics are similar to the above case.

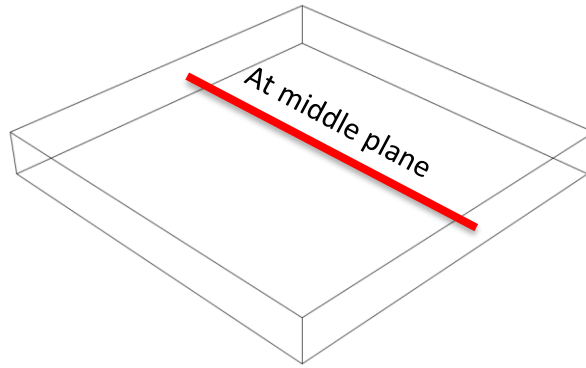


Figure 4.16: Path drawn at Inside of  $\text{Al}_2\text{O}_3$  nano particle Adhesive for peel stress and shear stress results

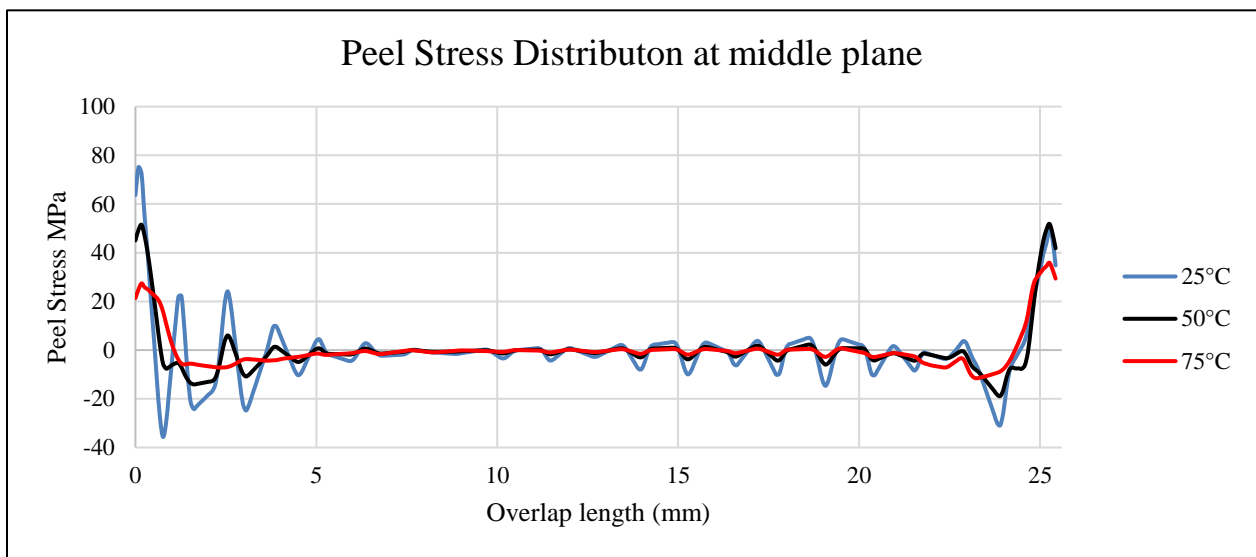


Figure 4.17: Peel Stress distribution at middle plane of adhesive with  $\text{Al}_2\text{O}_3$  nano particles at different temperatures

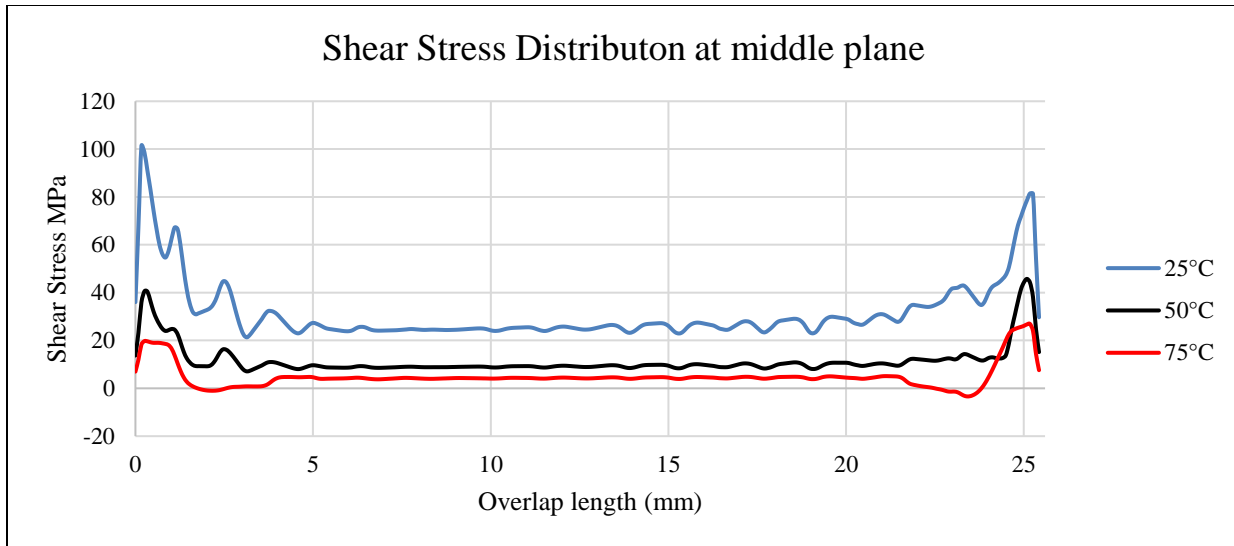


Figure 4.18: Shear Stress distribution at middle plane of adhesive with  $Al_2O_3$  nano particle at different temperatures

#### 4.2.3. At the longer edge of adhesive (along length)

Results for peel stress and shear stress along the length side of adhesive is given in the figure . The peak peel stress and shear stress is low at this location compared to the previous locations. The peak peel stresses are 64 MPa, 37 MPa, and 12 MPa at 25°C, 50°C, and 75°C respectively. Whereas the peak shear stresses are 59 MPa, 25 MPa, and 6 MPa at 25°C, 50°C, and 75°C temperature respectively. The peeling of adhesive is occurring at the end of the adhesive region and as the stress goes down to the middle of the region it approaches zero stress or minimum.

The mechanics for the joint at this location is not quite different with above cases but there are some differences. Highlighting the main difference which is the drop in Peak peel stress and the behavior of neat adhesive at higher temperature. The peak peel stress is dropped to 64 MPa at room temperature. Moreover, from the figure 4. the peak stress is 0.7 mm inside the adhesive from the edge at 25C but the peak peel stress at 50C and 75C it is at the edge. As the temperature decreased the stiffness in the adhesive is decreased drastically.



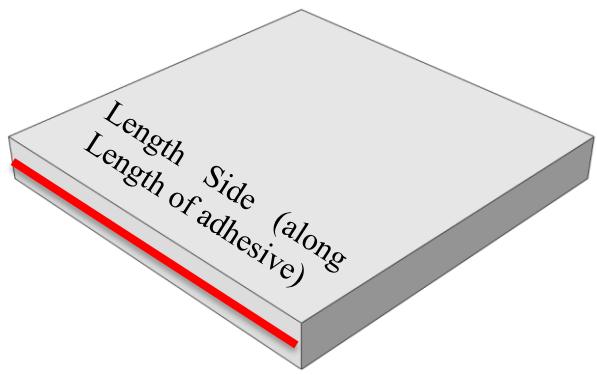


Figure 4.19: Path drawn at the longer edge of Al<sub>2</sub>O<sub>3</sub> nano particles- Adhesive for peel stress and shear stress results

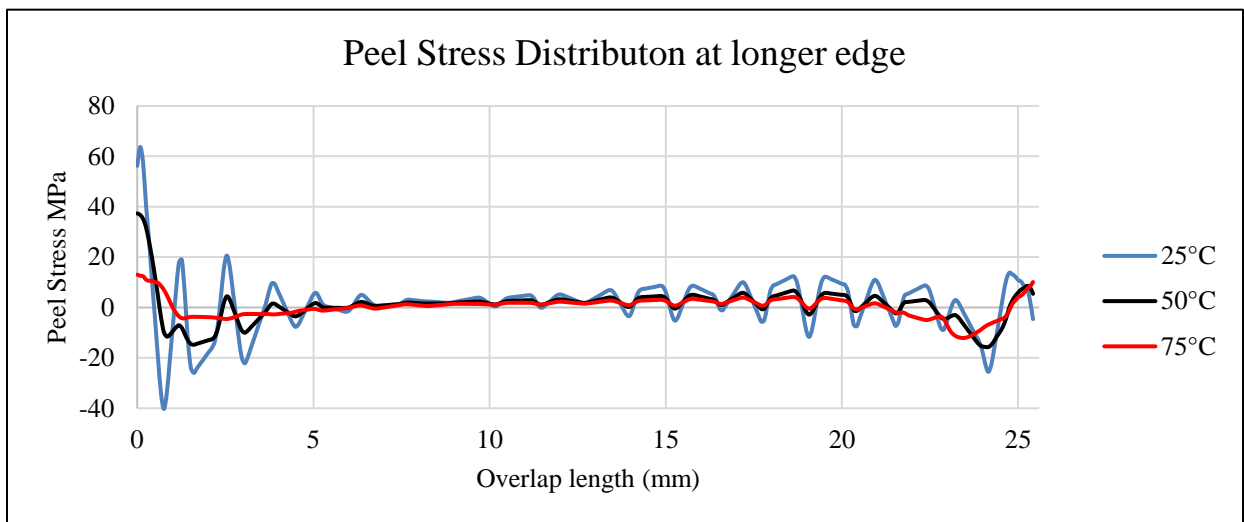


Figure 4.20: Peel Stress distribution at the longer edge of adhesive with Al<sub>2</sub>O<sub>3</sub> nano particles at different temperatures

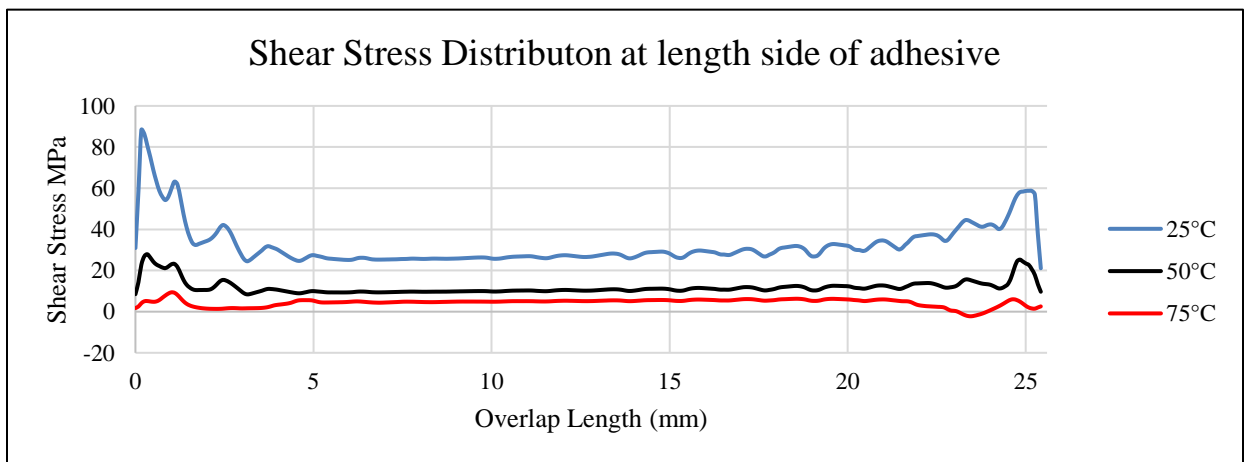


Figure 4.21: Shear Stress distribution at the longer edge of adhesive with Al<sub>2</sub>O<sub>3</sub> nano particle at different temperatures

#### 4.2.4. At the Shorter Edge of Adhesive (along width)

The results of peel stresses and shear stresses at this location is completely different from the previous cases. Both peel and shear stresses low at edges and climb to higher value at the middle of the side and then show a decreasing trend. peak values for Peel Stress are 36 MPa, 39 MPa and 27 MPa at 25°C, 50°C, and 75°C respectively with percentage increase of 8% in the peak value of peel stress for temperature increase from 25°C to 50°C. Whereas the value decreased by 30% at 75°C. The peak values for Shear Stresses are 29 MPa, 15 MPa and 7.5 MPa at 25°C, 50°C, and 75°C respectively. The peak value decrease as the temperature increased. 48% for 25°C to 50°C and 50% for 50°C to 75°C.

Considering the mechanics of the joint for this case, it is same as other cases in terms of decreasing trend with increase in temperature. At this location as the tensile load is applied, the material tries to move towards the center of the adhesive. The adhesive resists more at the center to deform than at the edges. It is because there is no material attached to the adhesive at the edges. Which results in lower peel stress at the edges and higher peel stress at the middle.

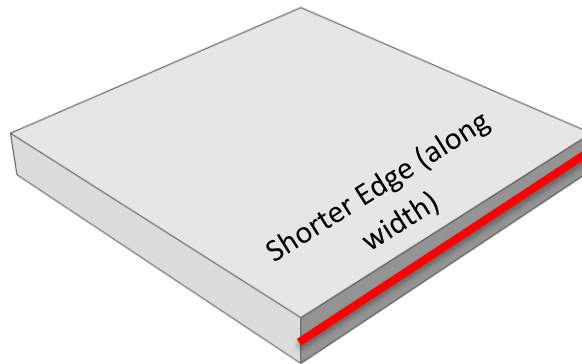


Figure 4.22: Path drawn at Shorter Edge of Adhesive for peel stress and shear stress results

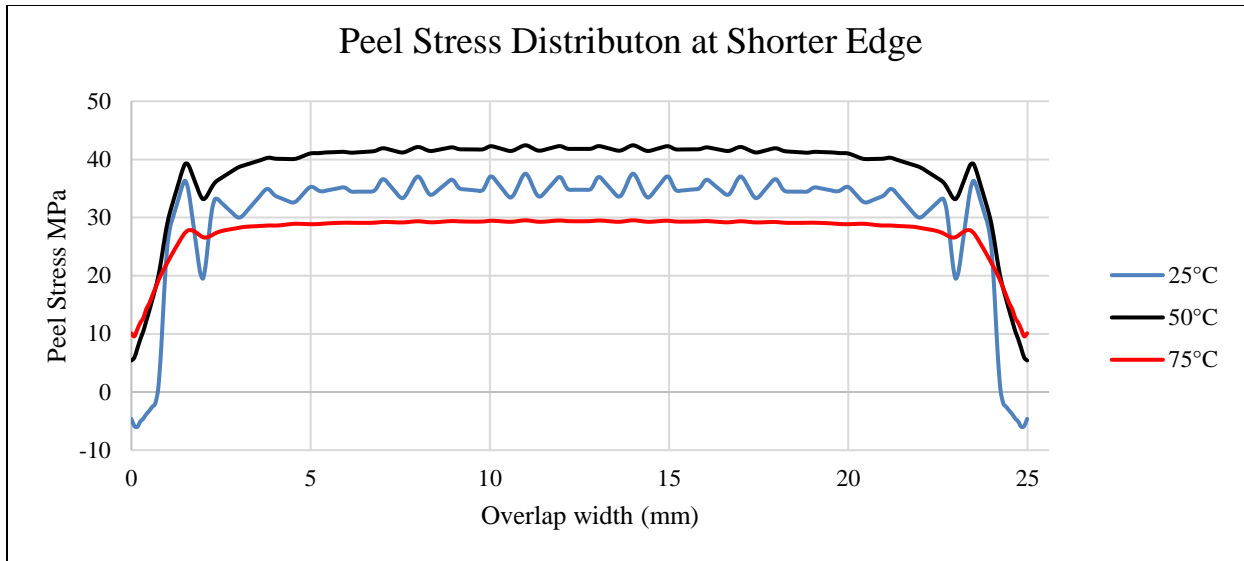


Figure 4.23: Peel Stress distribution at the shorter edge of adhesive with Al<sub>2</sub>O<sub>3</sub> nano particles at different temperatures

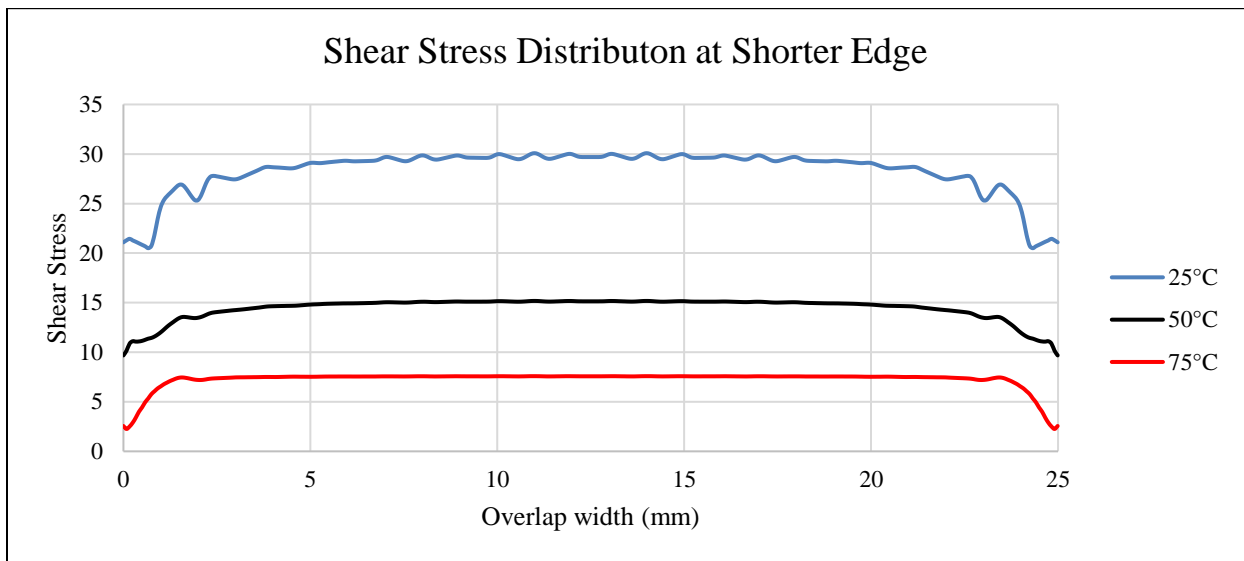


Figure 4.24: Shear Stress distribution at shorter edge of adhesive with Al<sub>2</sub>O<sub>3</sub> nano particle at different temperatures

### 4.3. Comparison between Neat and Nano filler Adhesive

In this section a comparative analysis between the results of neat adhesive and adhesive with alumina oxide. If the general mechanics and behavior to the tensile loading for both cases are

taken, they are quite similar. For example, in both cases the joint experience tensile and compressive stresses around the ends of the adhesive and as we go along to the center the peel stress reaches zero. Similarly, the shear stress results have the same pattern for both cases.

From the ref. [56] and [55] it was analyzed that added aluminum oxide  $\text{Al}_2\text{O}_3$  nano particles makes the adhesive stiff with high elastic modulus and it also increase the strength of the adhesive. The table 4.1 is showing a comprehensive comparison between peel stress, shear stress after adding 1.5wt% of  $\text{Al}_2\text{O}_3$  nano particles into the neat adhesive at different temperatures. Analyzing the table, it shows that by adding the nano particles at  $25^\circ\text{C}$  the peel stress decrease by 2% which signifies that adhesive material become less stiff. The peak peel and peak shear stress has reduced after inclusion of the  $\text{Al}_2\text{O}_3$  nano particles. This reduces the chance of early failure in the adhesive. moreover, as the peak stresses are at the ends of the adhesive which incurs that failure is will start from the end and travels toward the center, but it will not happen as early as it would in the case of neat adhesive due to  $\text{Al}_2\text{O}_3$  nano particles. As adhesive is analyzed at  $50^\circ\text{C}$  and  $75^\circ\text{C}$ , the addition of  $\text{Al}_2\text{O}_3$  nano particles has shown promising results. The peak peel and shear stress has increased 6.7% and 11.3% respectively compared to the stresses of neat adhesive. this shows that the adhesive has become stiff at higher temperatures and can be used at elevated temperatures. In the section 4.1, it was discussed that how the neat adhesive has behaved at  $50^\circ\text{C}$  and  $75^\circ\text{C}$ . the stresses were very low which signifies very low resistance to application of force that incurs the adhesive was not suitable to use at high temperature. But this problem can be solved using 1.5wt% of  $\text{Al}_2\text{O}_3$  nano particles with Epocast 50-A1 adhesive.

The shear stress occurs when adjacent layers move in the opposite directions when tensile load is applied. From the table 4.1, it can be seen that change in the shear stress has increased more at  $75^\circ\text{C}$  when  $\text{Al}_2\text{O}_3$  nano particles are added to neat adhesive. this shows that in tensile load the at  $75^\circ\text{C}$  the adhesive will show resistance to the load unlike in case of neat adhesive. this allows the adhesive to be used at elevated temperature.

To make it more understandable, figures of the locations where the results are focused, are attached along with the table.

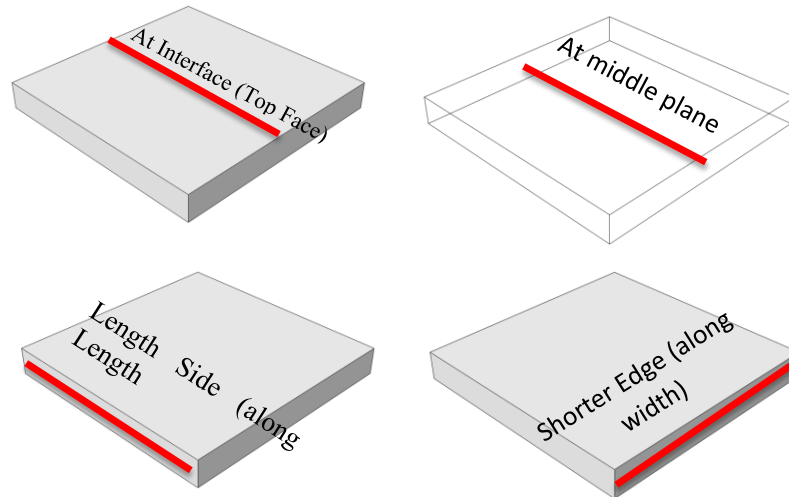


Figure 4.25: Geometrical locations of adhesive where results are focused

Table 4-1: Comparison of Percentage Change in Peel stress and Shear Stress with inclusion of 1.5wt% Al<sub>2</sub>O<sub>3</sub> Nanoparticles in Epocast 50-A1 Adhesive

<b>Top Face (Interface)</b>			
	<b>25°C</b>	<b>50°C</b>	<b>75°C</b>
<b>Peel Stress MPa (Max)</b>	-1.3398%	2.7226%	10.7377%
<b>Shear Stress MPa (Max)</b>	-19.6558%	7.7067%	8.7237%
<b>Middle Plane</b>			
<b>Peel Stress MPa (Max)</b>	-2.7024%	5.7714%	11.4387%
<b>Shear Stress MPa (Max)</b>	-19.4544%	4.9637%	9.2144%
<b>Longer Edge (Along Length)</b>			
<b>Peel Stress MPa (Max)</b>	-0.7977%	6.7663%	21.2440%
<b>Shear Stress MPa (Max)</b>	-20.7155%	9.0585%	23.8276%

Shorter Edge (Along Width)			
Peel Stress MPa (Max)	1.7025%	-4.7509%	-0.2935%
Shear Stress MPa (Max)	-4.1597%	7.1483%	14.4204%

**4.3.1. Graphical Comparison of Peel Stress between Neat and Al<sub>2</sub>O<sub>3</sub> nanoparticles Adhesive**

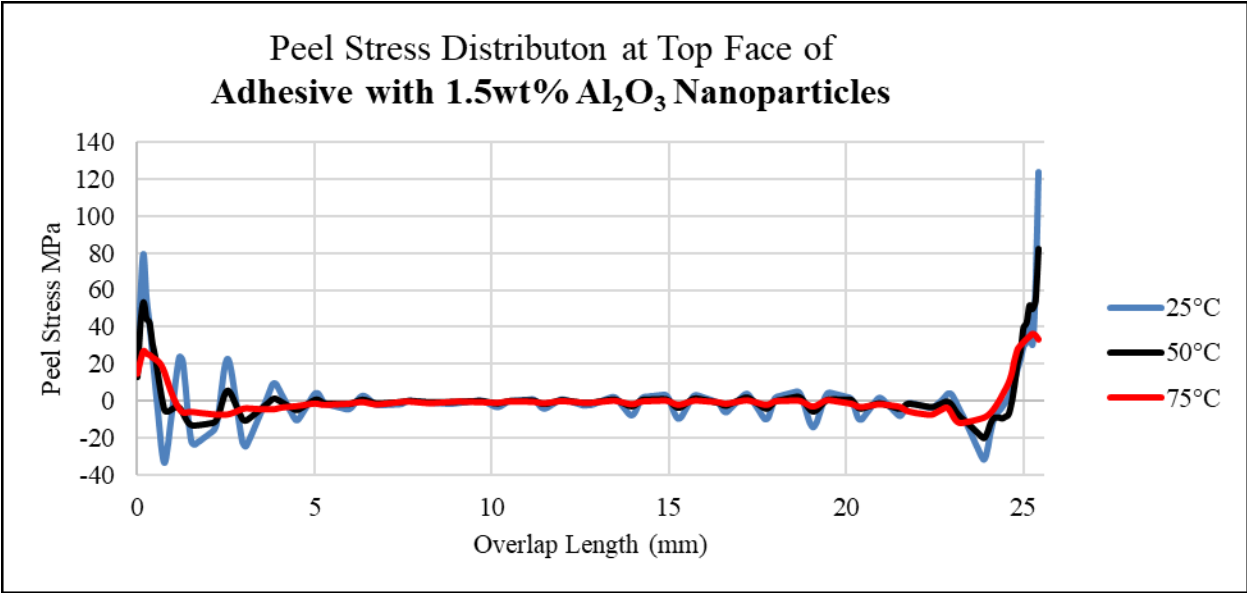
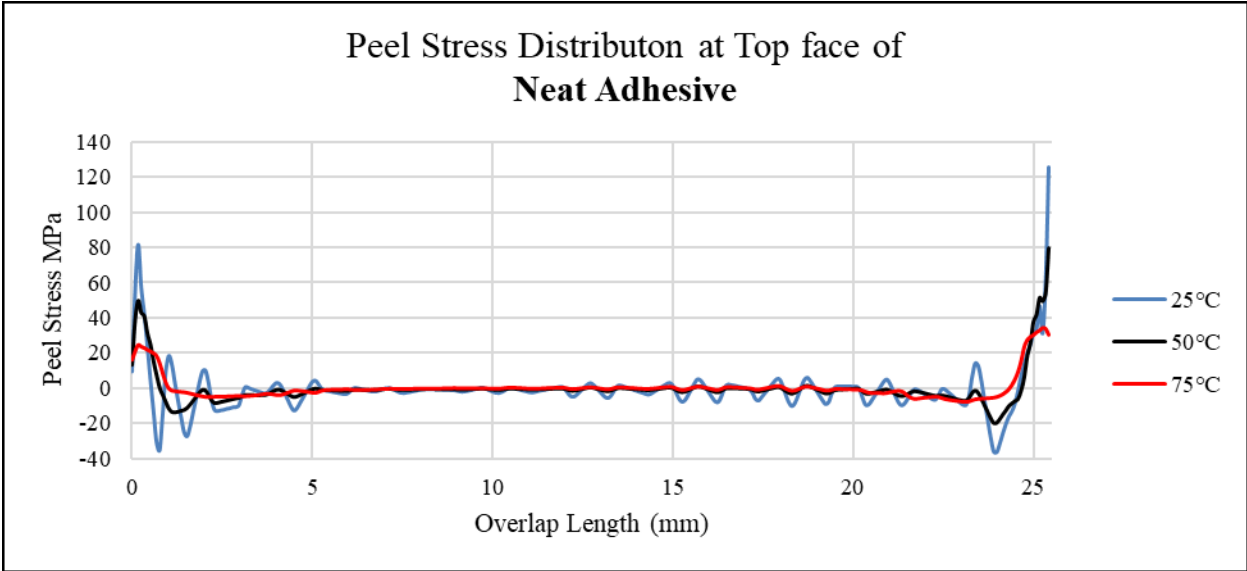


Figure 4.26: Comparison of Peel Stress of Neat and Al<sub>2</sub>O<sub>3</sub> Nanoparticles Adhesive at Top Face

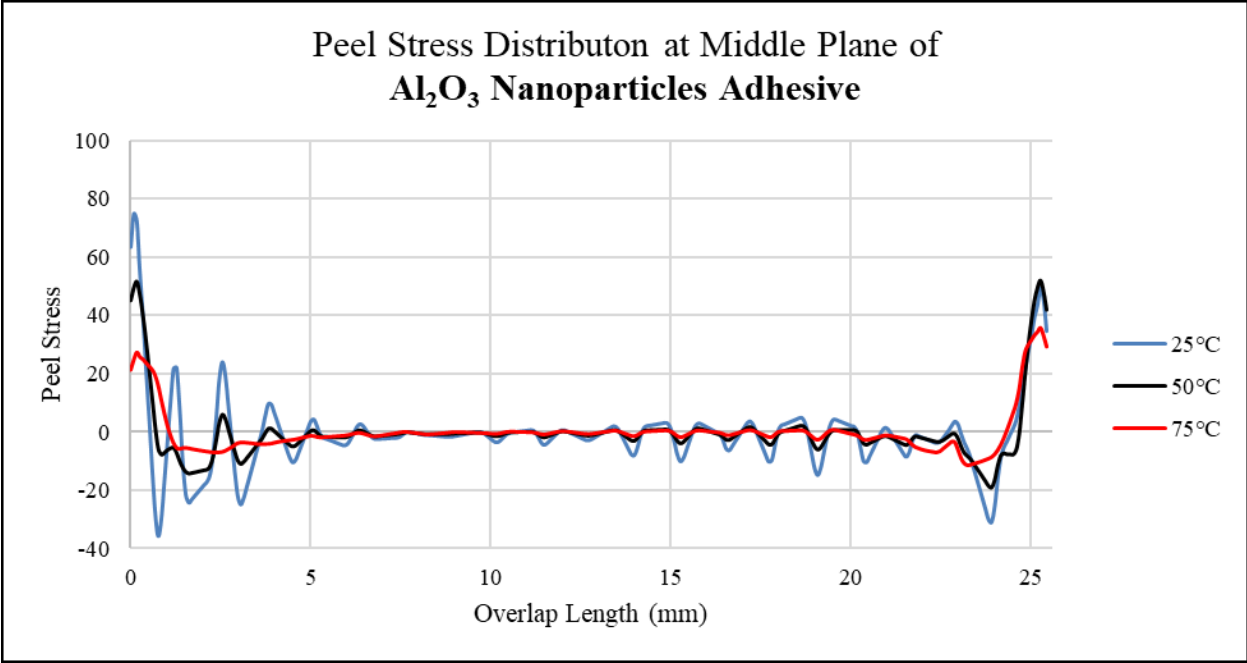
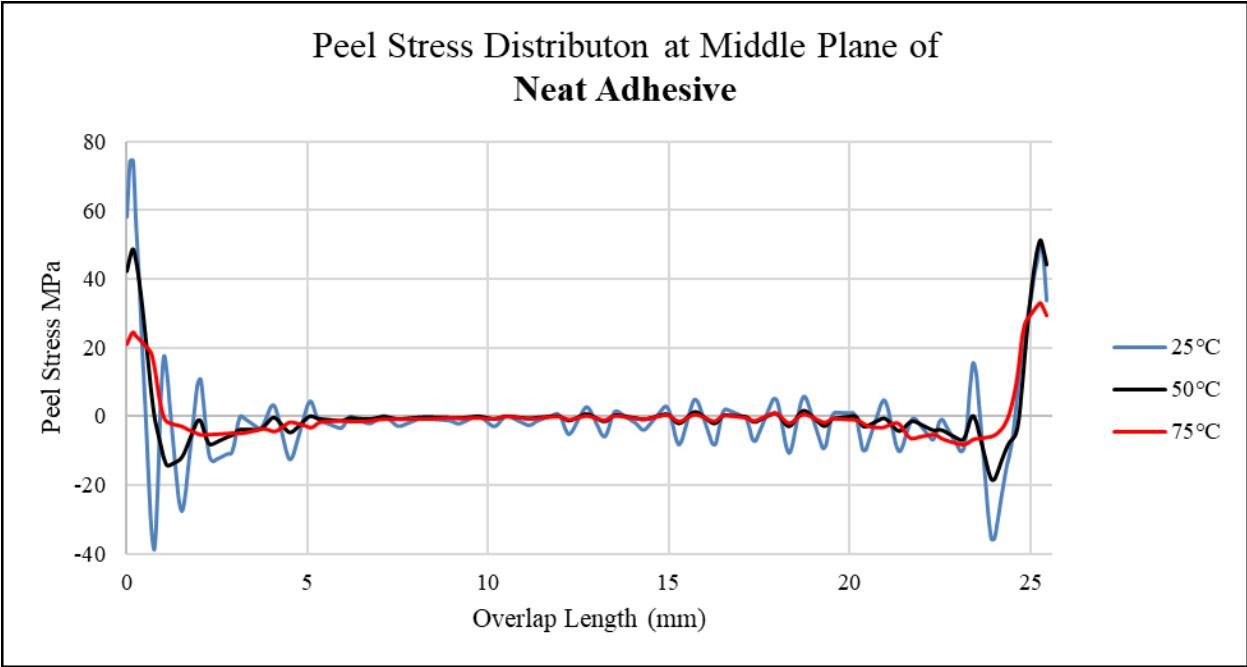


Figure 4.27: Comparison of Peel Stress of Neat and Al<sub>2</sub>O<sub>3</sub> Nanoparticles Adhesive at Middle Plane

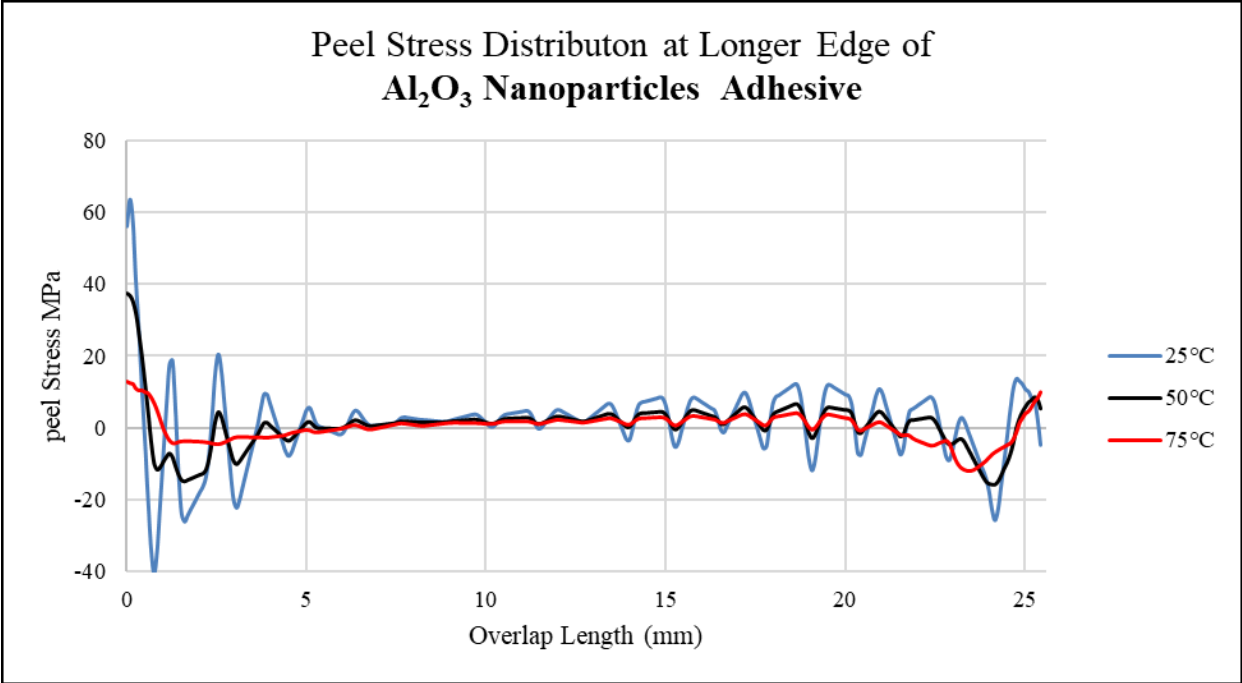
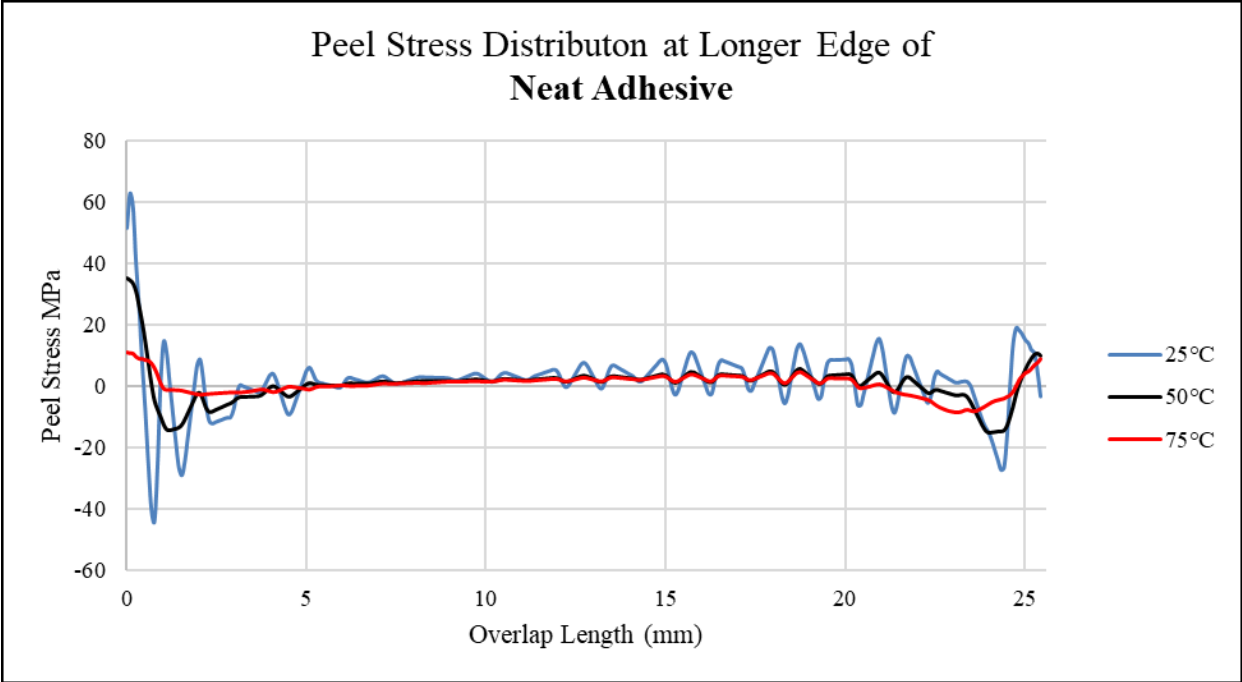


Figure 4.28: Comparison of Peel Stress of Neat and Al<sub>2</sub>O<sub>3</sub> Nanoparticles Adhesive at Longer Edge (Along Length)



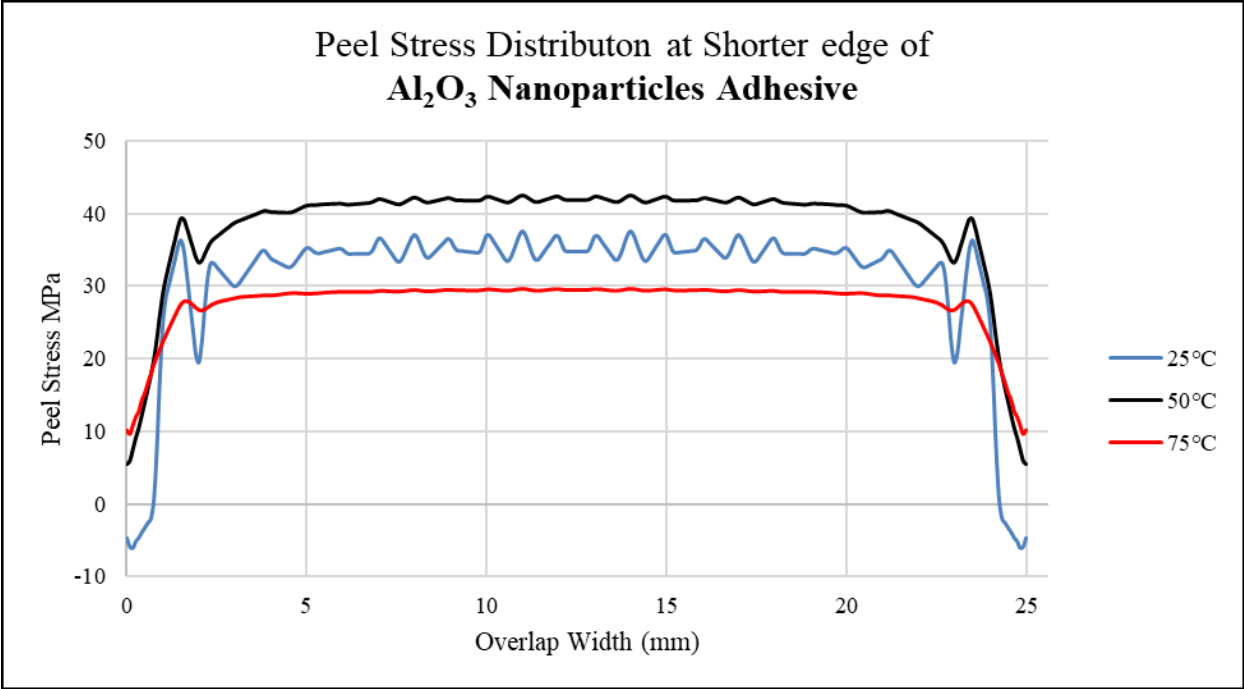
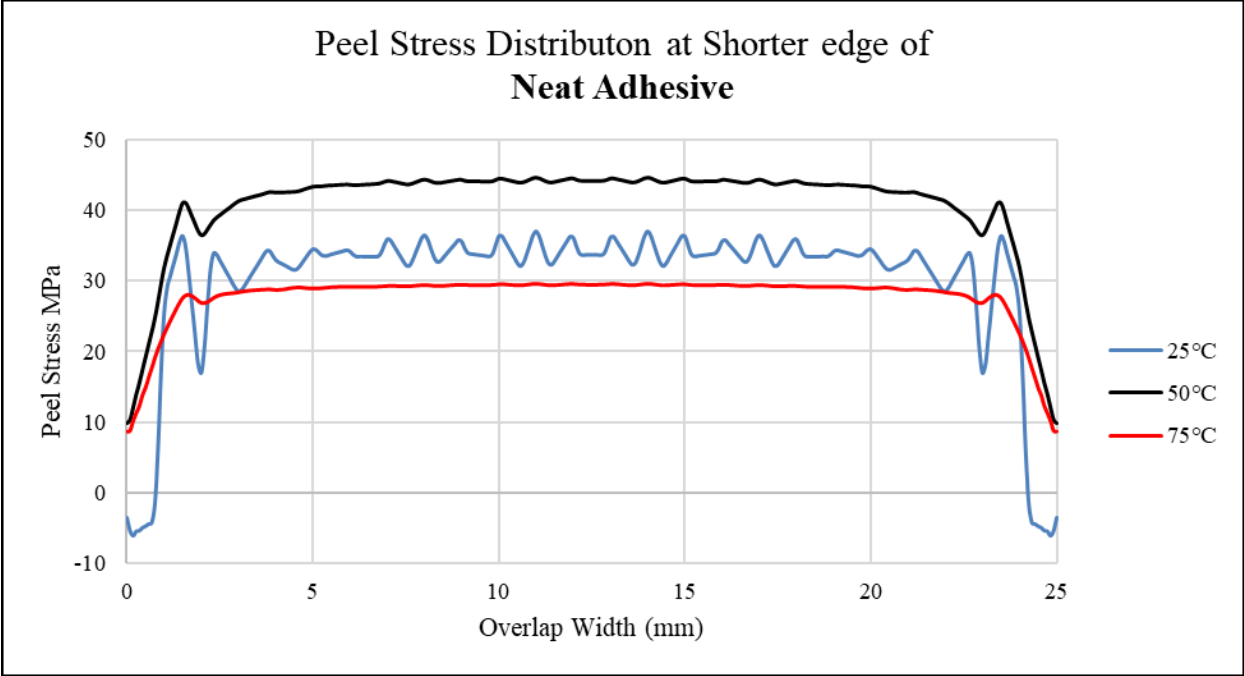


Figure 4.29: Comparison of Peel Stress of Neat and Al<sub>2</sub>O<sub>3</sub> Nanoparticles Adhesive at Shorter Edge (Along Width)

#### 4.3.2. Graphical Comparison of Shear Stress between Neat and Al<sub>2</sub>O<sub>3</sub> nanoparticles Adhesive

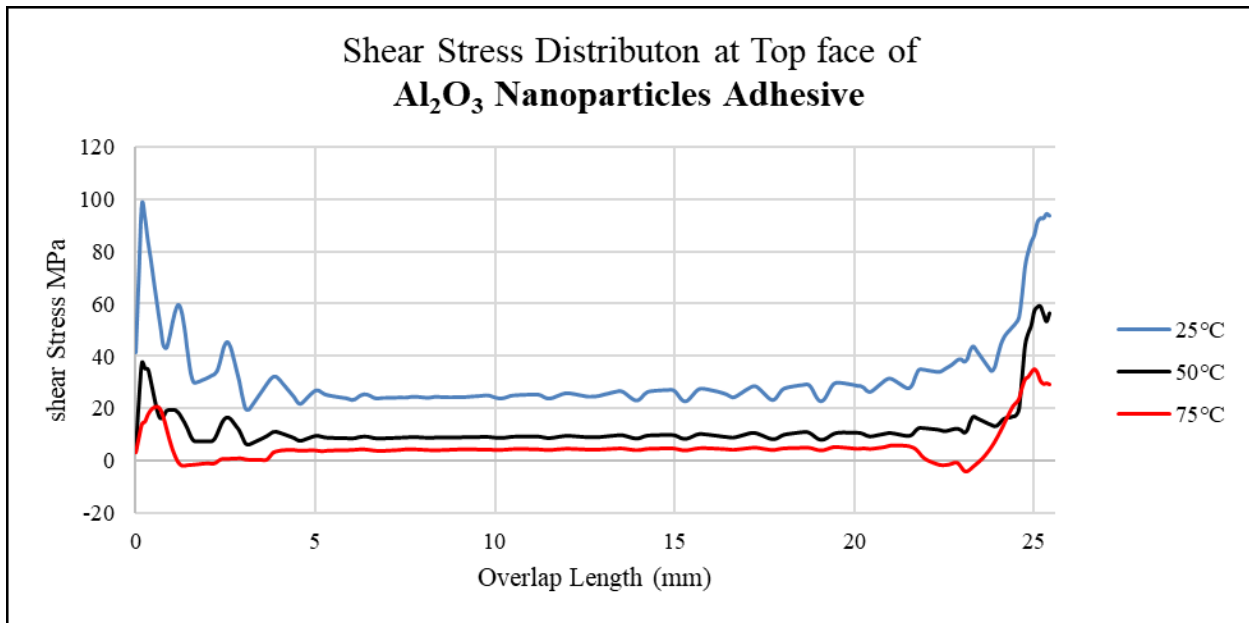
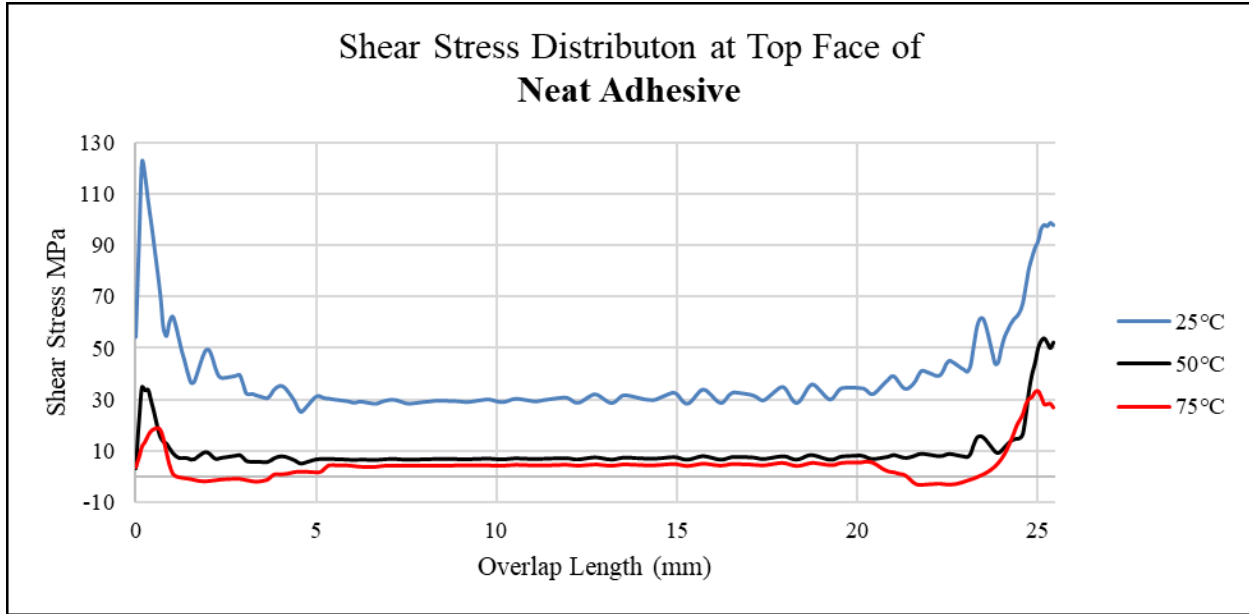


Figure 4.30: Comparison of Shear Stress of Neat and Al<sub>2</sub>O<sub>3</sub> Nanoparticles Adhesive at Top Face

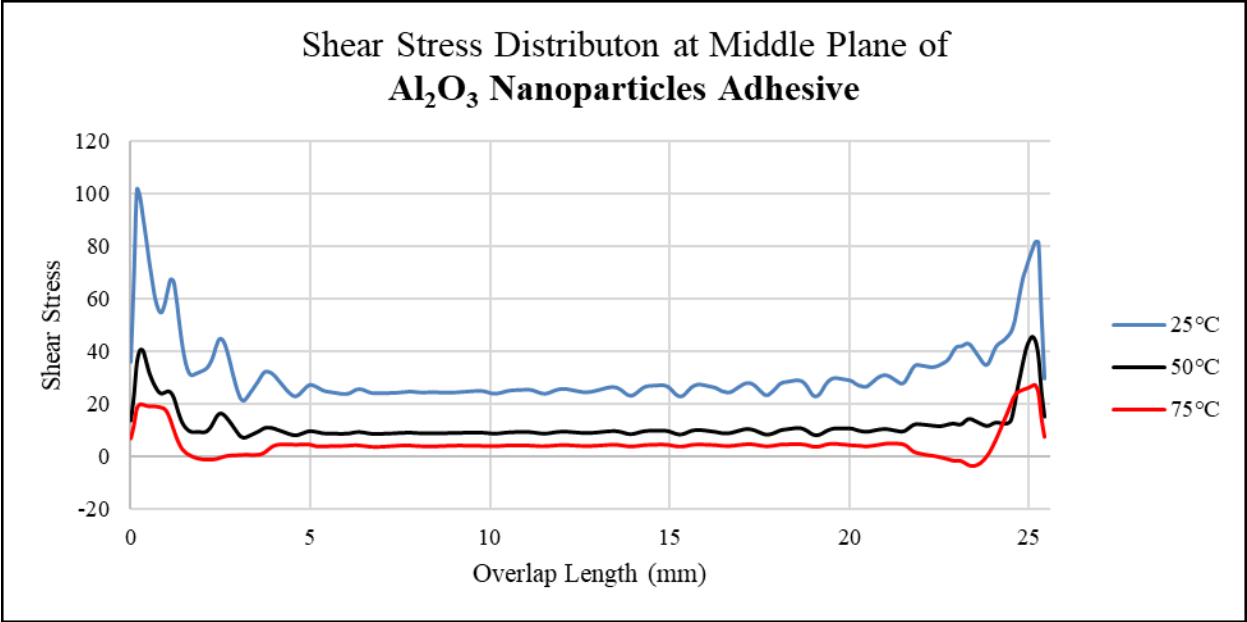
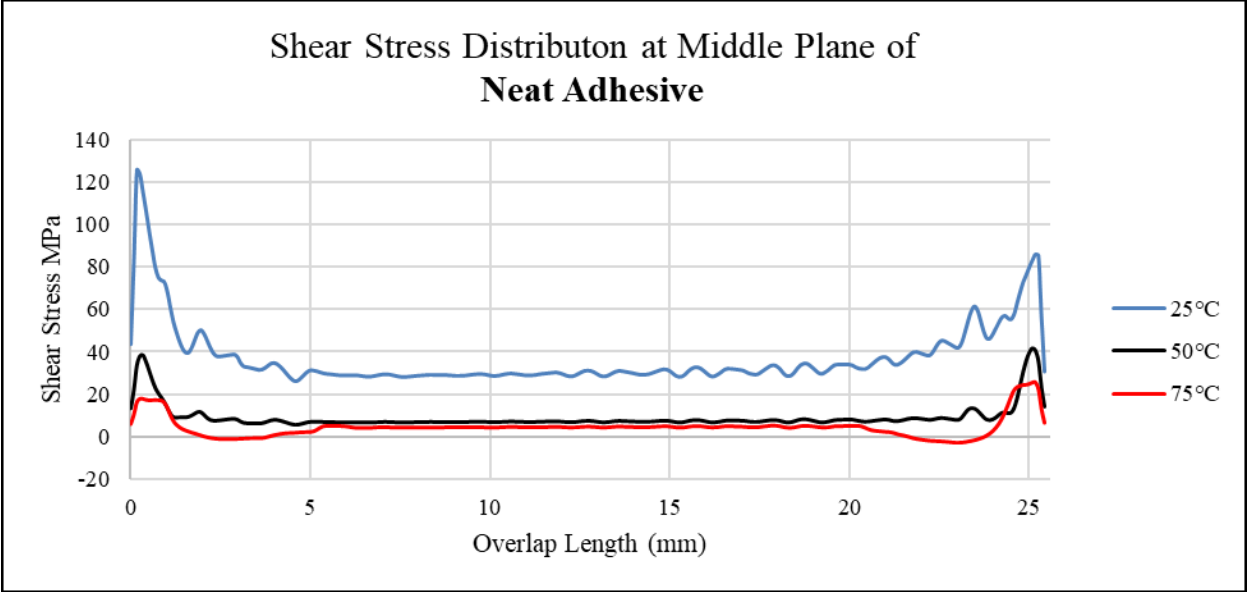


Figure 4.31: Comparison of Shear Stress of Neat and Al<sub>2</sub>O<sub>3</sub> Nanoparticles Adhesive at Middle Plane

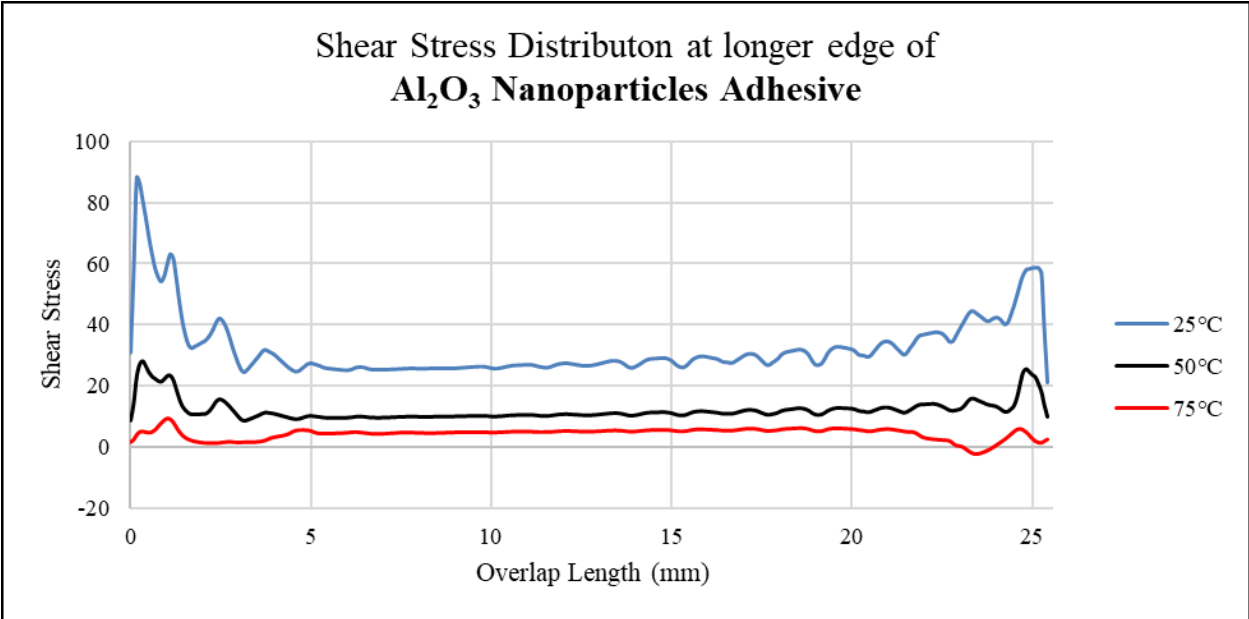
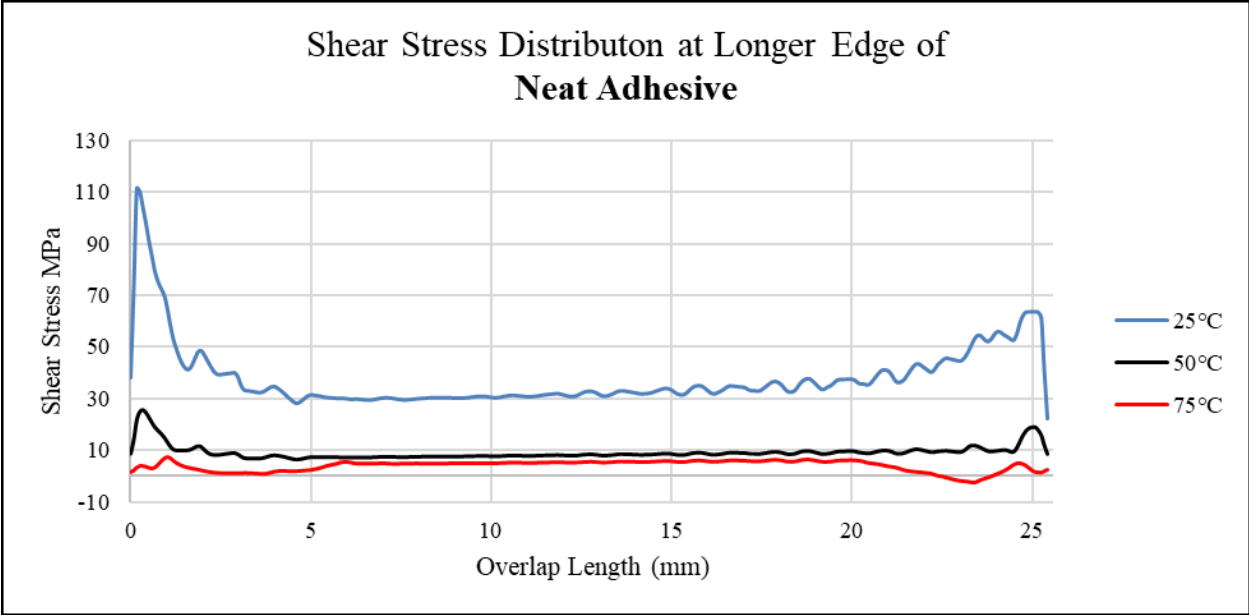


Figure 4.32: Comparison of Shear Stress of Neat and Al<sub>2</sub>O<sub>3</sub> Nanoparticles Adhesive at Longer Edge (Along Length)

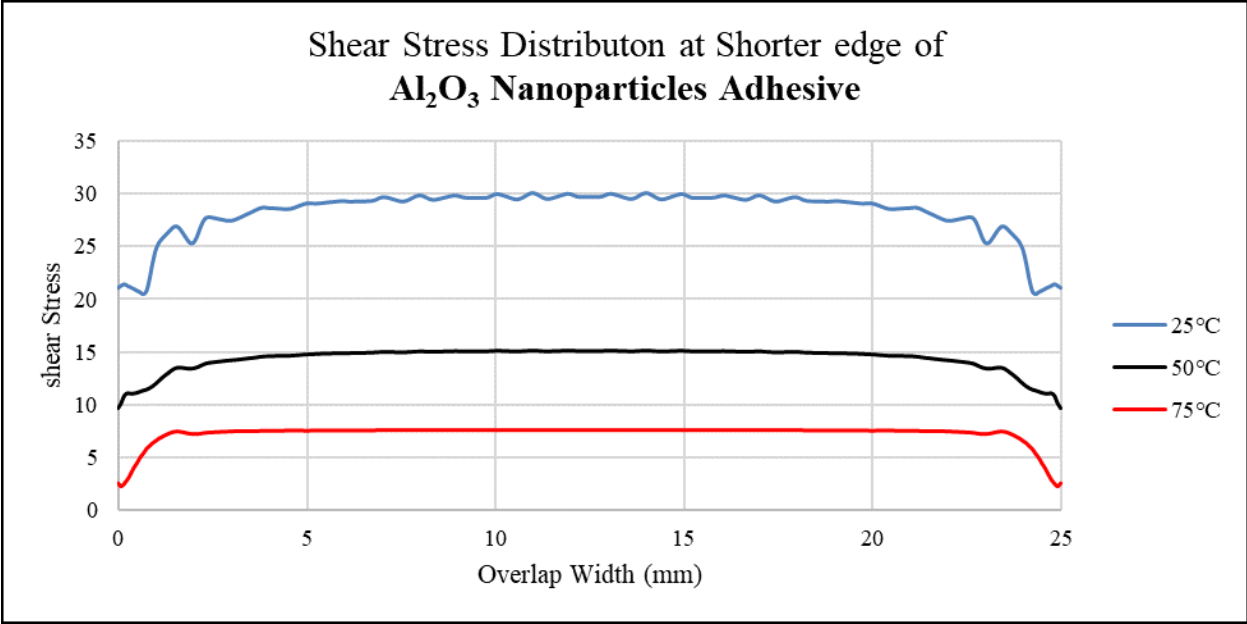
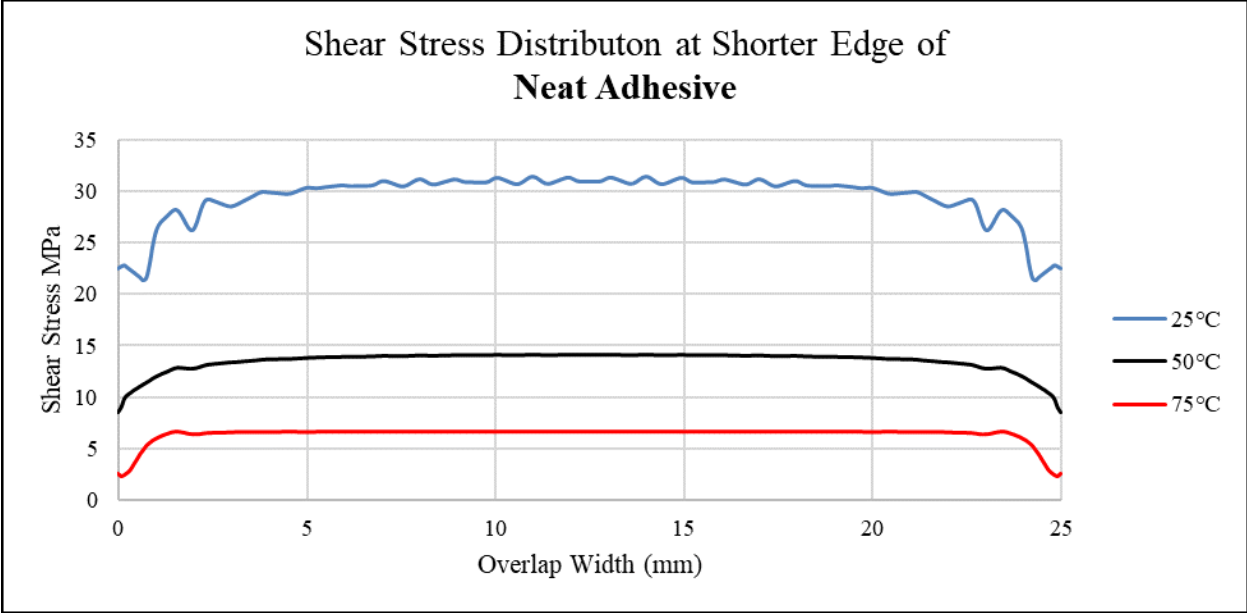


Figure 4.33: Comparison of Shear Stress of Neat and Al<sub>2</sub>O<sub>3</sub> Nanoparticles Adhesive at Shorter Edge (Along Width)

## Chapter 5: Conclusion and Future Work

### 5.1. Conclusion

In this study, peel stress and shear stress were analyzed at four different locations on the adhesive of a three-dimensional Single Lap Joint having two different kinds of adherends: one was composite carbon fiber, and the other was aluminum adherend. The Epocast 50-A1/946 epoxy was used as a neat adhesive and 1.5wt% Aluminum Oxide  $Al_2O_3$  nanoparticles were added to the epoxy to analyze the change in the elastic behavior of the adhesive. The SLJ was analyzed at three different temperatures 25°C, 50°C, and 75°C to observe the effect of temperature on the stresses and elastic behavior of neat and nanoparticle added adhesive.

It was concluded that adding  $Al_2O_3$  nanoparticles into the adhesive improved the properties of the epoxy at higher temperatures. This was evident from the rise in peel stress at the locations. This indicates that compared to neat adhesive, there was more resistance to tensile loading at 50°C and 75°C temperature hence adding stiffness to the adhesive. From the study, it was also analyzed that the adhesive of SLJ experiences higher stresses near the edges seeing the joint perpendicular to the length dimension. From this observation, it was concluded that the crack will initiate at the interface of adherend and adhesive close to the edge at both ends. The crack will then translate towards the center of the adhesive.

Stating the statistics at the interface location for using adhesive with  $Al_2O_3$  nanoparticles showed that peel stress and shear stress decreased by 1.3% and 19% respectively at 25°C. Shows that adhesive will behave less stiff than neat adhesive which will be beneficial for holding against more force than neat adhesive. The peel and shear stress showed an increase of 2.7% and 7.7 at 50°C and 10.7% and 8.7% at 75°C respectively. This concludes that the adhesive gets stiffer at a higher temperature compared to the neat adhesive. This shows that the adhesive will stand against more force than the neat adhesive due to the increase in stiffness.

## **5.2. Future Work**

1. The Finite Element Analysis results of this study needs experimental validation.
2. Failure analysis using Cohesive Zone Modeling CZM of the single lap joint used in this study.

## REFERENCES

- [1] K. DeVries and D. O. Adams, "Mechanical testing of adhesive joints," *Chapter*, vol. 6, pp. 193-234, 2002.
- [2] R. D. S. G. Campilho, M. De Moura, D. Ramantani, J. Morais, and J. Domingues, "Tensile behaviour of three-dimensional carbon-epoxy adhesively bonded single-and double-strap repairs," *International Journal of Adhesion and Adhesives*, vol. 29, no. 6, pp. 678-686, 2009.
- [3] J. Li, Y. Yan, T. Zhang, and Z. Liang, "Experimental study of adhesively bonded CFRP joints subjected to tensile loads," *International Journal of Adhesion and Adhesives*, vol. 57, pp. 95-104, 2015.
- [4] M. Kłonica, "Analysis of the effect of selected factors on the strength of adhesive joints," in *IOP Conference Series: Materials Science and Engineering*, 2018, vol. 393, no. 1, p. 012041: IOP Publishing.
- [5] S. A. Shaikh, Nitinkumar & Kanase, Pravin & Patil, Ajinkya & Tarate, Suraj, "Single Lap Adhesive Joint (SLAJ): A Study," *International Journal of Engineering and Technology*, pp. 64-70, 2017.
- [6] M. P. Lempke, "A STUDY OF SINGLE-LAP JOINTS," Mechanical Engineering – Master of Science, Michigan State University, 2013.
- [7] M. R. A. A. Akhavan-Safar, S. A. Bahreinian & L. F. M. da Silva, "Application of adhesively bonded single lap joints for fracture assessment of adhesive materials.," *The Journal of Adhesion*, vol. 95:1, pp. 1-22, 2019.
- [8] N. Barbosa, R. Campilho, F. Silva, and R. Moreira, "Comparison of different adhesively-bonded joint types for mechanical structures," *Applied Adhesion Science*, vol. 6, no. 1, pp. 1-19, 2018.
- [9] M. D. Banea, L. F. da Silva, and R. D. Campilho, "Principles of adhesive bonding," *Joining of Polymer-Metal Hybrid Structures: Principles and Applications*, pp. 3-27, 2018.
- [10] J. Renart, J. Costa, C. Sarrado, S. Budhe, A. Turon, and A. Rodríguez-Bellido, "Mode I fatigue behaviour and fracture of adhesively-bonded fibre-reinforced polymer (FRP) composite joints for structural repairs," in *Fatigue and Fracture of Adhesively-Bonded Composite Joints*: Elsevier, 2015, pp. 121-147.
- [11] J. Na, W. Mu, G. Qin, W. Tan, and L. Pu, "Effect of temperature on the mechanical properties of adhesively bonded basalt FRP-aluminum alloy joints in the automotive industry," *International Journal of Adhesion and Adhesives*, vol. 85, pp. 138-148, 2018.
- [12] Z. Ahmadi, "Nanostructured epoxy adhesives: A review," *Progress in Organic Coatings*, vol. 135, pp. 449-453, 2019.
- [13] G. Scarselli, C. Corcione, F. Nicassio, and A. Maffezzoli, "Adhesive joints with improved mechanical properties for aerospace applications," *International Journal of Adhesion and Adhesives*, vol. 75, pp. 174-180, 2017.



- [14] D. Alves, R. Campilho, R. Moreira, F. Silva, and L. Da Silva, "Experimental and numerical analysis of hybrid adhesively-bonded scarf joints," *International Journal of Adhesion and Adhesives*, vol. 83, pp. 87-95, 2018.
- [15] C. Watson, "Engineering Design with adhesives," in *Handbook of Adhesion* by D. E. Packham, J. W. Sons, Ed., 2005.
- [16] D. G. DIXON, "Aerospace applications of adhesives," in *Handbook of Adhesion* by D. E. Packham, J. W. Sons, Ed., 2005.
- [17] A. J. Kinloch, *Adhesion and adhesives: science and technology*. Springer Science & Business Media, 1987.
- [18] R. D. Adams, J. Comyn, and W. C. Wake, *Structural adhesive joints in engineering*. Springer Science & Business Media, 1997.
- [19] J. Shields, *Adhesives Handbook*, 3rd ed. ed. London: Butterworth, 1984.
- [20] S. Ebnesajjad, *ADHESIVES TECHNOLOGY HANDBOOK*. William Andrew, Norwich, NY, USA, 2008.
- [21] A. Ö. Lucas F. M. da Silva, Robert D. Adams, *Handbook of Adhesion Technology*, 2nd ed. Springer-Verlag Berlin Heidelberg, 2011.
- [22] J. Kuczmaszewski, *Fundamentals of metal-metal adhesive joint design*. Lublin University of Technology 2006.
- [23] E. M. Moya-Sanz, I. Ivañez, and S. K. Garcia-Castillo, "Effect of the geometry in the strength of single-lap adhesive joints of composite laminates under uniaxial tensile load," *International Journal of Adhesion and Adhesives*, vol. 72, pp. 23-29, 2017.
- [24] W. Guo, P. Chen, L. Yu, G. Peng, Y. Zhao, and F. Gao, "Numerical analysis of the strength and interfacial behaviour of adhesively bonded joints with varying bondline thicknesses," *International Journal of Adhesion and Adhesives*, vol. 98, p. 102553, 2020.
- [25] P. Chen, W. Guo, Y. Zhao, E. Li, Y. Yang, and H. Liu, "Numerical analysis of the strength and interfacial properties of adhesive joints with graded adherends," *International Journal of Adhesion and Adhesives*, vol. 90, pp. 88-96, 2019.
- [26] R. Adams and N. Peppiatt, "Stress analysis of adhesive-bonded lap joints," *Journal of strain analysis*, vol. 9, no. 3, pp. 185-196, 1974.
- [27] R. Adams and J. Harris, "The influence of local geometry on the strength of adhesive joints," *International Journal of Adhesion and Adhesives*, vol. 7, no. 2, pp. 69-80, 1987.
- [28] J. Ferreira, R. Campilho, M. Cardoso, and F. Silva, "Numerical simulation of adhesively-bonded T-stiffeners by cohesive zone models," *Procedia Manufacturing*, vol. 51, pp. 870-877, 2020.
- [29] J. Liu, T. Sawa, and H. Toratani, "A two-dimensional stress analysis and strength of single-lap adhesive joints of dissimilar adherends subjected to external bending moments," *The Journal of Adhesion*, vol. 69, no. 3-4, pp. 263-291, 1999.
- [30] R. Adams, R. Atkins, J. Harris, and A. Kinloch, "Stress analysis and failure properties of carbon-fibre-reinforced-plastic/steel double-lap joints," *The Journal of Adhesion*, vol. 20, no. 1, pp. 29-53, 1986.

- [31] M. Sandu, A. Sandu, D. M. Constantinescu, and D. A. Apostol, "Single-strap adhesively bonded joints with square or tapered adherends in tensile test conditions," *International Journal of Adhesion and Adhesives*, vol. 44, pp. 105-114, 2013.
- [32] L. F. Da Silva and M. J. C. Lopes, "Joint strength optimization by the mixed-adhesive technique," *International Journal of Adhesion and Adhesives*, vol. 29, no. 5, pp. 509-514, 2009.
- [33] K. Naito, M. Onta, and Y. Kogo, "The effect of adhesive thickness on tensile and shear strength of polyimide adhesive," *International journal of adhesion and adhesives*, vol. 36, pp. 77-85, 2012.
- [34] L. Sun, C. Li, Y. Tie, Y. Hou, and Y. Duan, "Experimental and numerical investigations of adhesively bonded CFRP single-lap joints subjected to tensile loads," *International Journal of Adhesion and Adhesives*, vol. 95, p. 102402, 2019.
- [35] H. Araújo, J. Machado, E. Marques, and L. Da Silva, "Dynamic behaviour of composite adhesive joints for the automotive industry," *Composite Structures*, vol. 171, pp. 549-561, 2017.
- [36] M. Banea, M. Rosioara, R. Carbas, and L. Da Silva, "Multi-material adhesive joints for automotive industry," *Composites Part B: Engineering*, vol. 151, pp. 71-77, 2018.
- [37] R. D. Campilho, M. De Moura, and J. Domingues, "Modelling single and double-lap repairs on composite materials," *Composites Science and Technology*, vol. 65, no. 13, pp. 1948-1958, 2005.
- [38] S. Wang, W. Liang, L. Duan, G. Li, and J. Cui, "Effects of loading rates on mechanical property and failure behavior of single-lap adhesive joints with carbon fiber reinforced plastics and aluminum alloys," *The International Journal of Advanced Manufacturing Technology*, vol. 106, no. 5, pp. 2569-2581, 2020.
- [39] M. Morgado, R. Carbas, D. Dos Santos, and L. Da Silva, "Strength of CFRP joints reinforced with adhesive layers," *International Journal of Adhesion and Adhesives*, vol. 97, p. 102475, 2020.
- [40] W. Mu, G. Qin, J. Na, W. Tan, H. Liu, and J. Luan, "Effect of alternating load on the residual strength of environmentally aged adhesively bonded CFRP-aluminum alloy joints," *Composites Part B: Engineering*, vol. 168, pp. 87-97, 2019.
- [41] M. Ostapiuk and J. Bienias, "Fracture Analysis and Shear Strength of Aluminum/CFRP and GFRP Adhesive Joint in Fiber Metal Laminates," *Materials*, vol. 13, no. 1, p. 7, 2020.
- [42] P. N. Reis, J. Ferreira, and F. Antunes, "Effect of adherend's rigidity on the shear strength of single lap adhesive joints," *International Journal of Adhesion and Adhesives*, vol. 31, no. 4, pp. 193-201, 2011.
- [43] T. Ribeiro, R. Campilho, L. F. da Silva, and L. Goglio, "Damage analysis of composite-aluminium adhesively-bonded single-lap joints," *Composite Structures*, vol. 136, pp. 25-33, 2016.
- [44] J. Korta, A. Mlyniec, and T. Uhl, "Experimental and numerical study on the effect of humidity-temperature cycling on structural multi-material adhesive joints," *Composites Part B: Engineering*, vol. 79, pp. 621-630, 2015.

- [45] R. Jairaja and G. N. Naik, "Single and dual adhesive bond strength analysis of single lap joint between dissimilar adherends," *International Journal of Adhesion and Adhesives*, vol. 92, pp. 142-153, 2019.
- [46] A. Rahmani and N. Choupani, "Experimental and numerical analysis of fracture parameters of adhesively bonded joints at low temperatures," *Engineering Fracture Mechanics*, vol. 207, pp. 222-236, 2019.
- [47] M. Adamvalli and V. Parameswaran, "Dynamic strength of adhesive single lap joints at high temperature," *International Journal of Adhesion and Adhesives*, vol. 28, no. 6, pp. 321-327, 2008.
- [48] T.-C. Nguyen, Y. Bai, R. Al-Mahaidi, and X.-L. Zhao, "Time-dependent behaviour of steel/CFRP double strap joints subjected to combined thermal and mechanical loading," *Composite Structures*, vol. 94, no. 5, pp. 1826-1833, 2012.
- [49] A. Rahmani, N. Choupani, and H. Kurtaran, "Thermo-fracture analysis of composite-aluminum bonded joints at low temperatures: experimental and numerical analyses," *International Journal of Adhesion and Adhesives*, vol. 95, p. 102422, 2019.
- [50] I. Ashcroft, D. Hughes, S. Shaw, M. A. Wahab, and A. Crocombe, "Effect of temperature on the quasi-static strength and fatigue resistance of bonded composite double lap joints," *The Journal of Adhesion*, vol. 75, no. 1, pp. 61-88, 2001.
- [51] F. Taheri, "Improvement of the Performance of Structural Adhesive Joints with Nanoparticles and Numerical Prediction of Their Response," *Structural Adhesive Joints: Design, Analysis and Testing*, pp. 35-78, 2020.
- [52] U. Khashaba, A. Aljinaidi, and M. Hamed, "Analysis of adhesively bonded CFRE composite scarf joints modified with MWCNTs," *Composites Part A: Applied Science and Manufacturing*, vol. 71, pp. 59-71, 2015.
- [53] U. Khashaba, "Dynamic analysis of scarf adhesive joints in CFRP composites modified with Al<sub>2</sub>O<sub>3</sub>-nanoparticles under fatigue loading at different temperatures," *Composites Part A: Applied Science and Manufacturing*, vol. 143, p. 106277, 2021.
- [54] A. Dorigato and A. Pegoretti, "The role of alumina nanoparticles in epoxy adhesives," *Journal of Nanoparticle Research*, vol. 13, no. 6, pp. 2429-2441, 2011.
- [55] S. K. Gupta, D. K. Shukla, and A. Bharti, "Effect of alumina nanoparticles on shear strength of epoxy adhesive: experimental and finite element analysis," in *2017 International Conference on Advances in Mechanical, Industrial, Automation and Management Systems (AMIAMS)*, 2017, pp. 307-313: IEEE.
- [56] U. Khashaba, A. Aljinaidi, and M. Hamed, "Nanofillers modification of Epocast 50-A1/946 epoxy for bonded joints," *Chinese Journal of Aeronautics*, vol. 27, no. 5, pp. 1288-1300, 2014.
- [57] C. Salom, M. Prolongo, A. Toribio, A. Martínez-Martínez, I. A. de Cárcer, and S. Prolongo, "Mechanical properties and adhesive behavior of epoxy-graphene nanocomposites," *International Journal of Adhesion and Adhesives*, vol. 84, pp. 119-125, 2018.
- [58] Y. Muqbool, "Effect of Temperature and Filler Concentration on the strength of adhesively bonded Single Lap joints.," Masters, Department of Mechanical Engineering, National

University of Science and Technology, School of Mechanical & Manufacturing Engineering, 2022.

- [59] Z. Taotao, L. Wenbo, X. Wei, and Y. Ying, "Numerical simulation of single-lap adhesive joint of composite laminates," *Journal of Reinforced Plastics and Composites*, vol. 37, no. 8, pp. 520-532, 2018.